PAPER

Theoretical and numerical studies of inverse source problem for the linear parabolic equation with sparse boundary measurements

To cite this article: Guang Lin et al 2022 Inverse Problems 38 125007

View the <u>article online</u> for updates and enhancements.

You may also like

- A tutorial on inverse problems for anomalous diffusion processes
 Bangti Jin and William Rundell
- A generalized quasi-boundary value method for recovering a source in a fractional diffusion-wave equation Ting Wei and Yuhua Luo
- Stability of an inverse source problem for the damped biharmonic plate equation Peijun Li, Xiaohua Yao and Yue Zhao

Theoretical and numerical studies of inverse source problem for the linear parabolic equation with sparse boundary measurements

Guang Lin^{1,*}, Zecheng Zhang² and Zhidong Zhang³

- Department of Mathematics and Mechanical Engineering, Purdue University, West Lafayette, IN 47906, United States of America
- ² Department of Mathematics, Purdue University, West Lafayette, IN 47906, United States of America
- ³ School of Mathematics (Zhuhai), Sun Yat-sen University, Zhuhai 519082, Guangdong, People's Republic of China

E-mail: guanglin@purdue.edu, zecheng.zhang.math@gmail.com and zhangzhidong@mail.sysu.edu.cn

Received 16 July 2022, revised 16 September 2022 Accepted for publication 13 October 2022 Published 1 November 2022



Abstract

We consider the inverse source problem in the parabolic equation, where the unknown source possesses the semi-discrete formulation. Theoretically, we prove that the flux data from any nonempty open subset of the boundary can uniquely determine the semi-discrete source. This means the observed area can be extremely small, and that is the reason we call it sparse boundary data. For the numerical reconstruction, we formulate the problem from the Bayesian sequential prediction perspective and conduct the numerical examples which estimate the space-time-dependent source state by state. To better demonstrate the method's performance, we solve two common multiscale problems from two models with a long source sequence. The numerical results illustrate that the inversion is accurate and efficient.

Keywords: inverse source problem, parabolic equation, sparse boundary measurements, uniqueness, numerical reconstruction

(Some figures may appear in colour only in the online journal)

^{*}Author to whom any correspondence should be addressed.

1. Introduction

1.1. Background and literature

As a classical type of PDEs, the parabolic equation is widely applied in physics, engineering, finance, and so on. The inverse source problems in the parabolic equation have various applications in the real world, and the corresponding research has a long history. We list representative work here [2, 13, 15–17, 26]. Denoting the unknown source by F(x, t), to recover it, we need the observations of the solution u on the whole domain $\mathbb{R}^d \times (0, \infty)$, which is impractical in almost every situation. Therefore, in the research of the inverse problem, people usually consider some special cases of unknown sources. For instance, a popular case is the variable separable source, i.e., F(x,t) := p(x)q(t). Given the spatial component p(x) or the temporal component q(t), recovering the other unknown part is a classical field in the inverse problems. See [3, 13, 14, 22] and the references therein. Furthermore, the work [23] considered the case when p(x) and q(t) are both unknown; in [17] the authors recovered the unknown source p(x',t) where $x' \in \mathbb{R}^{d-1}$. Compared with the variable separable form, the semi-discrete formulation below simulates the general source F(x,t) better:

$$F(x,t) := \sum_{k=1}^{K} p_k(x) \chi_{t \in [t_{k-1},t_k)}.$$

We can see the above formulation can approximate the general form F(x,t) accurately if the time mesh $\{0 \le t_0 < t_1 < \ldots\}$ is fine enough. The parabolic equation with a space-time-dependent source has many applications. For instance, in the area of medical research, one needs to trace the blood distribution in some tissues of the human body; in the reservoir simulation area, one example is to trace the amount of liquid injected into an oil field consisting of the impermeable rocks; in the ocean, people may need to determine the location of a leaking oil tanker and so on. In [19], the inverse source problem with the semi-discrete source is investigated.

In this work, the unknown source still has a semi-discrete formulation. The measurements we used are the boundary flux data, meaning the observed area will be the subset of the domain's boundary. To save cost, absolutely, we want the observed area to be as small as possible. In [19, 23], the authors considered the heat equation on the two-dimensional unit disc and proved the uniqueness theorem under the boundary flux data from two chosen points on the boundary. The proof depended on the explicit representation of the eigensystem of the Laplacian Δ on the two-dimensional unit disc. The conclusions in [19, 23] confirm that in the heat equation, if the domain has a smooth shape, then it is possible to recover the source from sparse boundary data. There is a natural question: can we solve a similar inverse source problem in the parabolic equation with a general domain, in which the explicit representation of the eigensystem is not applicable?

1.2. Mathematical statement and main theorem

We give the mathematical model as follows:

$$\begin{cases} (\partial_t + \mathcal{A})u(x,t) = \sum_{k=1}^K p_k(x)\chi_{t\in[t_{k-1},t_k)}, & (x,t) \in \Omega \times (0,\infty), \\ u(x,t) = 0, & (x,t) \in \partial\Omega \times (0,\infty) \cup \Omega \times \{0\}, \end{cases}$$

$$(1.1)$$

where $\Omega \subset \mathbb{R}^d$ is open and bounded. The operator \mathcal{A} is a symmetric elliptic operator, defined as

$$\mathcal{A}\psi = -\nabla \cdot (\kappa(x)\nabla\psi) + q(x)\psi, \quad \psi \in H^2(\Omega) \cap H_0^1(\Omega). \tag{1.2}$$

Here κ and q possess appropriate regularities to support the future proof, and they satisfy

$$0 < C_1 \le \kappa(x) \le C_2 < \infty$$
 and $q(x) \ge 0$ for a.e. $x \in \Omega$.

In the source term, the spatial components $\{p_k(x)\}_{k=1}^K$ and the time mesh $\{t_k\}_{k=0}^K$ are all undetermined. The measurements we used are the boundary flux data:

$$\frac{\partial u}{\partial \overrightarrow{\mathbf{n}}}(x,t), \quad (x,t) \in \Gamma \times (0,\infty) \subset \partial \Omega \times (0,\infty),$$

where $\overrightarrow{\mathbf{n}}$ means the outward normal unit vector of the boundary and $\Gamma \subset \partial \Omega$ is the observed area. Hence, the interesting inverse problem in this work is given as follows:

recovering
$$\{t_0, t_k, p_k(x)\}_{k=1}^K$$
 in the source from the data $\frac{\partial u}{\partial \overline{\mathbf{n}}}\Big|_{\Gamma \times (0,\infty)}$.

Remark 1.1. In the parabolic case, because of the analytic continuation, the data $\frac{\partial u}{\partial \overrightarrow{\mathbf{n}}}\big|_{\Gamma\times(0,\infty)}$ may be uniquely determined by $\frac{\partial u}{\partial \overrightarrow{\mathbf{n}}}\big|_{\Gamma\times(0,T)}$ with T>0. So we add this remark to explain why we use the measurements for $t\in(0,\infty)$. The proof of uniqueness in this work depends on corollary 3.2, which gives the relation between the measurements and unknowns. The convolution structure in the conclusion of corollary 3.2 implies us to use the Laplace transform. This is why we choose the data from $(0,\infty)$. See section 3 for details.

The approach in this work is more appropriate for the case of finite propagation speed, such as the wave equation. Since in such equations, the data from the finite time interval (0,T) cannot determine the unknown source uniquely. So that we may only start the proof from the data on $(0,\infty)$. The analogous inverse source problem in wave equation is one of our future works.

For this inverse problem, we have two goals: first, proving that the boundary flux data generated from a small observed area Γ can uniquely determine the source; second, recovering the unknown source from the sparse boundary data numerically. In the aspect of theoretical analysis, we attempt to build the uniqueness theorem. Firstly, we give some prior assumptions for the semi-discrete unknown source $\sum_{k=1}^K p_k(x)\chi_{t\in[t_{k-1},t_k)}$.

Assumption 1.2.

- (a) For the time mesh $\{t_k\}_{k=0}^K$, we have $K \in \mathbb{N}^+ \cup \{\infty\}$, and there exists $\eta > 0$ such that $\inf\{|t_k t_{k+1}| : k = 0, \dots, K 1\} \geqslant \eta$.
- (b) $\{p_k(x)\}_{k=1}^K \subset L^2(\Omega), \|p_k\|_{L^2(\Omega)} \neq 0 \text{ for } k=1,\ldots,K, \text{ and } \|p_k-p_{k+1}\|_{L^2(\Omega)} \neq 0 \text{ for } k=1,\ldots,K-1.$

In assumption 1.2(a), we do not require the time mesh $\{t_k\}_{k=0}^K$ be finite, which means K can be infinity. Also, assumption 1.2(b) is set to make sure the source $\sum_{k=1}^K p_k(x)\chi_{t\in[t_{k-1},t_k)}$ cannot be simplified further. Otherwise, if $\|p_{k_0}\|_{L^2(\Omega)} = \|p_{k_1-1} - p_{k_1}\|_{L^2(\Omega)} = 0$, then we can write the source as

$$\sum\nolimits_{k\notin\{k_0,k_1-1,k_1\}}p_k(x)\chi_{t\in[t_{k-1},t_k)}+p_{k_1}(x)\chi_{t\in[t_{k_1-2},t_{k_1})}.$$

In the next section, we will give assumption 2.4. With assumptions 1.2 and 2.4, we can state the main theorem of this work.

Theorem 1. Under assumptions 1.2 and 2.4, the flux data from any nonempty open subset of $\partial\Omega$ can uniquely determine the semi-discrete unknown source $\sum_{k=1}^{K} p_k(x) \chi_{t \in [t_{k-1},t_k)}$.

More precisely, given two sets of unknowns $\{t_0, t_k, p_k(x)\}_{k=1}^K$ and $\{\tilde{t}_0, \tilde{t}_k, \tilde{p}_k(x)\}_{k=1}^K$, we denote the corresponding solutions by u and \tilde{u} respectively, assume assumptions 1.2 and 2.4 be valid, and let $\Gamma \subset \partial \Omega$ be an arbitrary nonempty open subset. Provided

$$\left.\frac{\partial u}{\partial \, \overrightarrow{\mathbf{n}}}\right|_{\Gamma\times(0,\infty)} = \frac{\partial \widetilde{u}}{\partial \, \overrightarrow{\mathbf{n}}}\bigg|_{\Gamma\times(0,\infty)},$$

we have $\{t_0, t_k, p_k(x)\}_{k=1}^K = \{\tilde{t}_0, \tilde{t}_k, \tilde{p}_k(x)\}_{k=1}^{\tilde{K}}$.

Theorem 1 confirms that the data from any nonempty open subset of the boundary is sufficient to support the uniqueness of this inverse source problem.

1.3. Bayesian formulation and outline

After proving theorem 1 for this inverse source problem, it is time to consider reconstructing the unknown source numerically. The design of the algorithm will be challenging since there are too many unknowns in the source. The conventional methods are hard to handle problems with high dimensional unknowns and are very sensitive to the observation locations. However, from the semi-discrete formulation, one needs to estimate a sequence of unknown states $\{p_k(x)\}_{k=1}^K$ recursively in time. Hence, one natural idea is to estimate each state $p_k(x)$ given a sequence of observations up to k in time by the posterior distribution. This task of sequential prediction based on the online observations can then be categorized as the standard Bayesian filtering problem, which has been thoroughly studied in control theory [5, 10, 20, 24]. This motivates us to formulate the inversion problem in the Bayesian framework.

The numerical reconstruction is a time series tracking problem and consists of constructing the posterior probability distribution of a sequence of states based on observations. The resulting model is typically highly nonlinear with non-Gaussian distribution, so obtaining an explicit exact solution is hard work. This reminds us of estimating the state recursively via a filtering approach [18]. In this work, we will use the particle filter (PF) algorithm to compute the posterior of the state in a sequence. The benefit of the PF algorithm is that it can handle any nonlinear properties and is capable to solve any distribution (no Gaussian assumption) [9, 25]. The PF algorithms usually involve sampling from a probabilistic model which depends on the previous states and observations. The samples are called particles and constitute an empirical approximation of the model. The trajectories are then extended by sampling the following state particles based on the existing particles and new observations. The degeneration issue is a concern of the PF algorithm, but the resampling techniques can reduce the variance of the particles. In this work, we use the systematical resampling [7, 9], and please check [7] for a comprehensive review of the resampling schemes. Another concern of the PF algorithms is the design of the proposal. Many techniques like linearization [8], extended Kalman filter, and unscented PF [25] are among the most important options to this issue. In this work, we use the transition prior, and the results are satisfactory. The details can be seen in section 4.

The contribution of this work can be summarized as follows:

(a) Prove the uniqueness theorem rigorously and confirm that the semi-discrete source can be recovered by the flux data from any nonempty open subset of the boundary. This conclusion can decrease the cost of real projects and is meaningful in practical applications.

(b) To solve the inverse problem numerically, we formulate the process as a sequential prediction and hence use the filter algorithm to predict the semi-discrete source. The method enables us to solve the models with a long sequence of states and is very accurate.

Finally, we give the outline of this paper. In section 2, we collect several useful results and show some lemmas which will be used in future proofs. In section 3 we will prove the main result—theorem 1. The proof depends on the Laplace transform and the knowledge of complex analysis. In section 4, we consider the numerical reconstruction of this inverse source problem. The algorithm is given, and some satisfactory numerical results are provided. In section 5, we list some future works for this inverse source problem.

2. Preliminaries

2.1. Eigensystem of A on Ω

For the operator $\mathcal A$ defined in (1.2), we denote the eigensystem by $\{\lambda_n, \varphi_n(x)\}_{n=1}^\infty$. Since $\mathcal A$ is positive definite and self-adjoint, we have that $0<\lambda_1\leqslant\lambda_2\leqslant\dots$ and $\lambda_n\to\infty$ as $n\to\infty$, and the set of eigenfunctions $\{\varphi_n(x)\}_{n=1}^\infty$ constitutes an orthonormal basis of the space $L^2(\Omega)$. Furthermore, if φ_n is an eigenfunction of $\mathcal A$ corresponding to λ_n , so is $\overline{\varphi_n}$. Here $\overline{\varphi_n}$ means the complex conjugate of φ_n . This gives that the set $\{\varphi_n(x)\}_{n=1}^\infty$ coincides with $\{\overline{\varphi_n(x)}\}_{n=1}^\infty$. Also, from the trace theorem, we have $\{\frac{\partial \varphi_n}{\partial \overline{\mathbf{n}}}|_{\partial\Omega}\}_{n=1}^\infty \subset H^{1/2}(\partial\Omega)$, and the next lemma concerns the non-vanishing property of $\frac{\partial \varphi_n}{\partial \overline{\mathbf{n}}}|_{\partial\Omega}$.

Lemma 2.1. If Γ is a nonempty open subset of $\partial\Omega$, then for each $n \in \mathbb{N}^+$, $\frac{\partial \varphi_n}{\partial \vec{\mathbf{n}}}$ cannot vanish almost everywhere on Γ .

Proof. Assume that there exists $k \in \mathbb{N}^+$ and a nonempty open subset $\Gamma \subset \partial \Omega$ such that $\frac{\partial \varphi_k}{\partial \overrightarrow{\mathbf{n}}} = 0$ a.e. on Γ . This implies that we can find r > 0 and $x_0 \in \partial \Omega$ such that $\frac{\partial \varphi_k}{\partial \overrightarrow{\mathbf{n}}} \equiv 0$ a.e. on $B(x_0, r) \cap \partial \Omega$, where $B(x_0, r)$ is the ball centered at x_0 with radius r in \mathbb{R}^d . Now define the extension Ω_e of Ω as $\Omega_e = \Omega \cup B(x_0, r)$ and the extended function $\varphi_{k,e}$ of φ_k on Ω_e as

$$\varphi_{k,e}(x) = \begin{cases} \varphi_k(x), & x \in \Omega, \\ 0, & x \in B(x_0, r) \setminus \Omega. \end{cases}$$

Obviously, $\varphi_{k,e} \in H^1(\Omega_e)$. Now for any $\psi \in C_c^{\infty}(\Omega_e)$, we have

$$\int_{\Omega_{e}} (\kappa \nabla \varphi_{k,e} \cdot \nabla \psi + q(x)\varphi_{k,e}\psi - \lambda_{k}\varphi_{k,e}\psi) dx$$

$$= \int_{\Omega} (\kappa \nabla \varphi_{k,e} \cdot \nabla \psi + q(x)\varphi_{k,e}\psi - \lambda_{k}\varphi_{k,e}\psi) dx + \int_{B(x_{0},r)\backslash\Omega} 0 dx$$

$$= \int_{\Omega} [(\mathcal{A} - \lambda_{k})\varphi_{k}]\psi dx = 0.$$

Hence, $\varphi_{k,e} \in H^1(\Omega_e)$ is a weak solution of the equation

$$(A - \lambda_k)v(x) = 0, \quad x \in \Omega_e,$$

and we can find $B(x_0',r')\subset B(x_0,r)\subset\Omega_e$ s.t. $\varphi_{k,e}\equiv 0$ on $B(x_0',r')$. By the unique continuation principle, we have $\varphi_{k,e}\equiv 0$ on Ω_e , i.e. φ_k vanishes on Ω , which contradicts with the fact that $\|\varphi_k\|_{L^2(\Omega)}=1$. Therefore we conclude that $\frac{\partial \varphi_k}{\partial \vec{\mathbf{n}}}$ does not vanish almost everywhere on any nonempty open subset of $\partial\Omega$, and the proof is complete.

2.2. The set $\{\xi_{l}\}_{l=1}^{\infty}$

In this part, we build the auxiliary set of functions $\{\xi_l\}_{l=1}^{\infty}$ which will be used later. For $\psi_1, \psi_2 \in L^2(\Omega), \psi_3, \psi_4 \in L^2(\partial\Omega)$, we define

$$\langle \psi_1, \psi_2 \rangle_{\Omega} = \int_{\Omega} \psi_1(\cdot) \overline{\psi_2(\cdot)} dx, \qquad \langle \psi_3, \psi_4 \rangle_{\kappa, \partial\Omega} = \int_{\partial\Omega} \kappa(\cdot) \psi_3(\cdot) \overline{\psi_4(\cdot)} dx,$$

and accordingly we give the induced norm $\|\cdot\|_{L^2(\Omega)}$, $\|\cdot\|_{L^2(\kappa,\partial\Omega)}$ as

$$\|\cdot\|_{L^2(\Omega)}^2 = \langle\cdot,\cdot\rangle_{\Omega}, \qquad \|\cdot\|_{L^2(\kappa,\partial\Omega)}^2 = \langle\cdot,\cdot\rangle_{\kappa,\partial\Omega}.$$

Not hard to see $\|\cdot\|_{L^2(\kappa,\partial\Omega)}$ is equivalent to the usual L^2 norm $\|\cdot\|_{L^2(\partial\Omega)}$. The next lemma considers a density property.

Lemma 2.2. For the eigenfunctions $\{\varphi_n\}_{n=1}^{\infty}$ defined in section 2.1, we have $\operatorname{Span}\{\frac{\partial \varphi_n}{\partial \overrightarrow{\pi}}|\partial\Omega\}_{n=1}^{\infty}$ is dense in $L^2(\kappa,\partial\Omega)$.

Proof. With the density of $H^{3/2}(\partial\Omega)$ in $L^2(\partial\Omega)$ under the norm $\|\cdot\|_{L^2(\partial\Omega)}$, it is sufficient to prove that $\tilde{\psi} \in H^{3/2}(\partial\Omega)$ vanishes almost everywhere on $\partial\Omega$ if $\langle \tilde{\psi}, \frac{\partial \varphi_n}{\partial \Pi} | \partial\Omega \rangle_{\kappa,\partial\Omega} = 0$ for each $n \in \mathbb{N}^+$.

We let ψ satisfy the following system:

$$\begin{cases} A\psi(x) = 0, & x \in \Omega, \\ \psi = \tilde{\psi}, & x \in \partial\Omega. \end{cases}$$

The regularity $\tilde{\psi} \in H^{3/2}(\partial\Omega)$ gives that $\psi \in H^2(\Omega)$, then the Green's identity can be used. Fixing one $n \in \mathbb{N}^+$, we have

$$\langle \mathcal{A}\psi, \varphi_n \rangle_{\Omega} - \langle \psi, \mathcal{A}\varphi_n \rangle_{\Omega} = \langle \tilde{\psi}, \frac{\partial \varphi_n}{\partial \overrightarrow{\mathbf{n}}} \rangle_{\kappa, \partial \Omega} - \langle \frac{\partial \psi}{\partial \overrightarrow{\mathbf{n}}}, \varphi_n \rangle_{\kappa, \partial \Omega}.$$

With the results $\mathcal{A}\psi=0$ on Ω , $\varphi_n=0$ on $\partial\Omega$ and $\langle \tilde{\psi}, \frac{\partial \varphi_n}{\partial \vec{\mathbf{n}}} \rangle_{\kappa,\partial\Omega}=0$, the above equality gives that

$$\langle \psi, \mathcal{A}\varphi_n \rangle_{\Omega} = \lambda_n \langle \psi, \varphi_n \rangle_{\Omega} = 0.$$

So we see that for each $n \in \mathbb{N}^+$, $\langle \psi, \varphi_n \rangle_{\Omega} = 0$. This together with the completeness of $\{\varphi_n\}_{n=1}^{\infty}$ in $L^2(\Omega)$ yields that $\|\psi\|_{L^2(\Omega)} = 0$. From the definition of the weak derivative, it is not hard to see that the first-order weak derivative of ψ is also vanishing on Ω . This gives that $\|\psi\|_{H^1(\Omega)} = 0$. By the continuity of the trace operator, it holds that

$$\|\psi|_{\partial\Omega}\|_{L^2(\partial\Omega)} = \|\tilde{\psi}\|_{L^2(\partial\Omega)} \leqslant C\|\psi\|_{H^1(\Omega)} = 0.$$

So we have $\tilde{\psi}=0$ almost everywhere on $\partial\Omega$ and the proof is complete.

Now we can build the auxiliary set $\{\xi_l\}_{l=1}^{\infty}$. With the density of $\mathrm{Span}\{\frac{\partial \varphi_n}{\partial \, \mathbf{n}}|_{\partial\Omega}\}_{n=1}^{\infty}$ in $L^2(\kappa,\partial\Omega)$, we can construct the orthonormal basis $\{\tilde{\xi}_l\}_{l=1}^{\infty}$ in $L^2(\kappa,\partial\Omega)$ as follows. Firstly, we set $\tilde{\xi}_1 = \frac{\partial \varphi_1}{\partial \, \mathbf{n}}|_{\partial\Omega}/\|\frac{\partial \varphi_1}{\partial \, \mathbf{n}}\|_{L^2(\kappa,\partial\Omega)}$, and for $l=2,3,\ldots$, we assume that the orthonormal set $\{\tilde{\xi}_j\}_{j=1}^{l-1}$ has been constructed. Then we let $n_l \in \mathbb{N}^+$ be the smallest number such that $\frac{\partial \varphi_{n_l}}{\partial \, \mathbf{n}}|_{\partial\Omega} \notin \mathrm{Span}\{\tilde{\xi}_j\}_{j=1}^{l-1}$, and after that we can pick $\tilde{\xi}_l \in \mathrm{Span}\{\frac{\partial \varphi_{n_l}}{\partial \, \mathbf{n}}|_{\partial\Omega}, \tilde{\xi}_1,\ldots,\tilde{\xi}_{l-1}\}$ such that

$$\langle \tilde{\xi}_l, \tilde{\xi}_j \rangle_{\kappa, \partial \Omega} = 0$$
 for $j = 1, \dots, l - 1$, $\|\tilde{\xi}_l\|_{L^2(\kappa, \partial \Omega)} = 1$.

The density of $\operatorname{Span}\{\frac{\partial \varphi_n}{\partial \overrightarrow{\mathbf{n}}}|_{\partial\Omega}\}_{n=1}^{\infty}$ in $L^2(\kappa,\partial\Omega)$ ensures that $\{\tilde{\xi}_l\}_{l=1}^{\infty}$ is an orthonormal basis in $L^2(\kappa,\partial\Omega)$. Also, from the smoothness property $\frac{\partial \varphi_n}{\partial \overrightarrow{\mathbf{n}}}|_{\partial\Omega} \in H^{1/2}(\partial\Omega)$ we have $\{\tilde{\xi}_l\}_{l=1}^{\infty} \subset H^{1/2}(\partial\Omega)$.

Next, for each $l \in \mathbb{N}^+$, let $\xi_l \in H^1(\Omega)$ be the weak solution of the following system:

$$\begin{cases} \mathcal{A}\xi_{l}(x) = 0, & x \in \Omega, \\ \xi_{l} = \tilde{\xi}_{l}, & x \in \partial\Omega. \end{cases}$$
 (2.1)

Then we get the auxiliary set $\{\xi_l\}_{l=1}^{\infty}$ on Ω

2.3. The coefficients $\{c_{z,n}\}$ and assumption 2.4

The proof of theorem 1 relies on assumption 2.4. Before stating assumption 2.4, we need to build the coefficients $\{c_{z,n}\}$. For a fixed point $z \in \partial\Omega$, we define the series $\psi_z^N \in H^1(\overline{\Omega})$ as

$$\psi_z^N(x) = \sum_{l=1}^N \tilde{\xi}_l(z) \overline{\xi_l(x)}, \quad x \in \overline{\Omega},$$
 (2.2)

where $\{\xi_l, \xi_l\}_{l=1}^{\infty}$ are defined in the above subsection. Then we consider the following system and denote the solutions by $\{u_{\tau}^N\}$:

$$\begin{cases} (\partial_t + \mathcal{A})u_z^N(x,t) = 0, & (x,t) \in \Omega \times (0,\infty), \\ u_z^N(x,t) = 0, & (x,t) \in \partial\Omega \times (0,\infty), \\ u_z^N(x,0) = -\psi_z^N, & x \in \Omega. \end{cases}$$
 (2.3)

The finite summation ψ_z^N is constructed following the role of the Dirac delta function, which reflects the information of the targeted function on a specific point via integration. With the following lemma, we can give the coefficients $\{c_{z,n}\}$.

Lemma 2.3. For each $z \in \partial \Omega$ and $n \in \mathbb{N}^+$, $\lim_{N \to \infty} \langle \psi_z^N, \overline{\varphi_n} \rangle_{\Omega}$ exists.

Proof. Firstly from Green's identities we have

$$\begin{split} \langle \psi_z^N, \overline{\varphi_n} \rangle_{\Omega} &= \lambda_n^{-1} \langle \psi_z^N, \mathcal{A} \overline{\varphi_n} \rangle_{\Omega} \\ &= \lambda_n^{-1} \bigg(\langle \mathcal{A} \psi_z^N, \overline{\varphi_n} \rangle_{\Omega} - \langle \psi_z^N, \frac{\partial \overline{\varphi_n}}{\partial \overrightarrow{\mathbf{n}}} \rangle_{\kappa, \partial \Omega} + \langle \frac{\partial \psi_z^N}{\partial \overrightarrow{\mathbf{n}}}, \overline{\varphi_n} \rangle_{\kappa, \partial \Omega} \bigg) \\ &= -\lambda_n^{-1} \sum_{l=1}^N \tilde{\xi}_l(z) \langle \frac{\partial \varphi_n}{\partial \overrightarrow{\mathbf{n}}}, \tilde{\xi}_l \rangle_{\kappa, \partial \Omega} =: c_{z,n}^N, \end{split}$$

where the system (2.1) and the boundary condition of φ_n are used. From the definition of $\{\tilde{\xi}_l\}_{l=1}^{\infty}$, we see that $\langle \frac{\partial \varphi_n}{\partial \vec{\mathbf{n}}}, \tilde{\xi}_l \rangle_{\kappa,\partial\Omega} = 0$ for large l. Hence, if N is sufficiently large, the value $\lambda_n^{-1} \sum_{l=1}^N \tilde{\xi}_l(z) \langle \frac{\partial \varphi_n}{\partial \overline{n}}, \tilde{\xi}_l \rangle_{\kappa, \partial \Omega}$ will not depend on the value of N. This means that $\lim_{N \to \infty} \langle \psi_z^N, \overline{\varphi_n} \rangle_{\Omega}$ exists, and the proof is complete.

Now we define,

$$c_{z,n} := \lim_{N \to \infty} \langle \psi_z^N, \overline{\varphi_n} \rangle_{\Omega} = \lim_{N \to \infty} c_{z,n}^N, \quad p_{k,n} := \langle p_k(\cdot), \varphi_n(\cdot) \rangle_{\Omega}, \tag{2.4}$$

it is time to state assumption 2.4.

Assumption 2.4.

- (a) For $k \in \{1, ..., K\}$ and a.e. $z \in \partial \Omega$, there exists C > 0 which is independent of N such that $\sum_{n=1}^{\infty} |c_{z,n}^N p_{k,n}| < C < \infty$ for each $N \in \mathbb{N}^+$.
- (b) For a.e. $z \in \partial \Omega$, it holds that $\sum_{k=1}^{K} \sum_{n=1}^{\infty} |c_{z,n}p_{k,n}| < \infty$. (c) For a.e. $t \in [0,\infty)$, the spatial components $\{p_k(x)\}_{k=1}^{K}$ are smooth enough such that the series $\sum_{l=1}^{\infty} \tilde{\xi}_l(x) \langle \frac{\partial u}{\partial \overline{\mathbf{n}}}(\cdot,t), \tilde{\xi}_l(\cdot) \rangle_{\kappa,\partial\Omega}$ converges to $\frac{\partial u}{\partial \overline{\mathbf{n}}}(x,t)$ point-wisely for a.e. $x \in \partial \Omega$.

3. Uniqueness theorem

3.1. Representation of the boundary flux data

In this part, we will consider how to present the boundary flux $\frac{\partial u}{\partial \mathbf{r}}|_{\partial\Omega}$ by the unknown source. Firstly, we give the next lemma.

Lemma 3.1. For a.e. $z \in \partial \Omega$, we define $w_z^N = u_z^N + \psi_z^N$, where u_z^N and ψ_z^N are given by (2.3) and (2.2), respectively. Then we have:

for a.e. $t \in [0, t_0]$,

$$-\frac{\partial u}{\partial \overrightarrow{\mathbf{n}}}(z,t)=0;$$

for a.e. $t \in (t_{m_0-1}, t_{m_0}]$ with $1 \le m_0 \le K$,

$$-\frac{\partial u}{\partial \overrightarrow{\mathbf{n}}}(z,t) = \lim_{N \to \infty} \int_{\Omega} p_{m_0}(x) w_z^N(x,t-t_{m_0-1}) dx$$

$$+ \sum_{m=1}^{m_0-1} \lim_{N \to \infty} \int_{\Omega} p_m(x) [w_z^N(x,t-t_{m-1}) - w_z^N(x,t-t_m)] dx;$$

for a.e. $t \in (t_K, \infty)$ (when K is finite),

$$-\frac{\partial u}{\partial \overrightarrow{\mathbf{n}}}(z,t) = \sum_{m=1}^K \lim_{N \to \infty} \int_{\Omega} p_m(x) [w_z^N(x,t-t_{m-1}) - w_z^N(x,t-t_m)] dx.$$

Proof. From the definition of ψ_z^N , we see that $(\partial_t + \mathcal{A})\psi_z^N = 0$. This result and (2.3) show that w_{τ}^{N} satisfies the equation

$$(\partial_t + \mathcal{A})w_z^N = 0, \quad (x, t) \in \Omega \times (0, \infty),$$

with the boundary condition $w_z^N|_{\partial\Omega}=\psi_z^N|_{\partial\Omega}$ and the initial condition $w_z^N(x,0)=0$. Therefore, Green's identities give that for each $v\in H^1_0(\Omega)$,

$$\int_{\Omega} (\partial_t + q) w_z^N(x, t) v(x) + \kappa(x) \nabla w_z^N(x, t) \cdot \nabla v(x) dx = 0, \quad t \in (0, \infty).$$

From (1.1), we obtain

$$\int_0^t \int_{\Omega} F(x,\tau) w_z^N(x,t-\tau) dx d\tau = \int_0^t \int_{\Omega} (\partial_t + \mathcal{A}) u(x,\tau) w_z^N(x,t-\tau) dx d\tau.$$

Green's identities and the vanishing initial conditions of u and w_z^N give that

$$\begin{split} \int_0^t \int_\Omega (\partial_t + q) u(x,\tau) w_z^N(x,t-\tau) \mathrm{d}x \ \mathrm{d}\tau &= \int_0^t \int_\Omega (\partial_t + q) w_z^N(x,t-\tau) u(x,\tau) \mathrm{d}x \, \mathrm{d}\tau, \\ \int_0^t \int_\Omega - \nabla \cdot (\kappa \nabla u(x,\tau)) w_z^N(x,t-\tau) \mathrm{d}x \ \mathrm{d}\tau &= \int_0^t \int_\Omega \kappa(x) \nabla u(x,\tau) \cdot \nabla w_z^N(x,t-\tau) \mathrm{d}x \, \mathrm{d}\tau \\ &- \int_0^t \int_{\partial\Omega} \kappa(x) \frac{\partial u}{\partial \overrightarrow{\mathbf{n}}}(x,\tau) \psi_z^N(x) \mathrm{d}x \, \mathrm{d}\tau. \end{split}$$

Hence, we have

$$\begin{split} &\int_0^t \int_{\Omega} F(x,\tau) w_z^N(x,t-\tau) \mathrm{d}x \, \mathrm{d}\tau \\ &= \int_0^t \int_{\Omega} (\partial_t + q) w_z^N(x,t-\tau) u(x,\tau) + \kappa(x) \nabla w_z^N(x,t-\tau) \cdot \nabla u(x,\tau) \mathrm{d}x \, \mathrm{d}\tau \\ &- \int_0^t \int_{\partial \Omega} \kappa(x) \frac{\partial u}{\partial \overrightarrow{\mathbf{n}}}(x,\tau) \psi_z^N(x) \mathrm{d}x \, \mathrm{d}\tau \\ &= - \int_0^t \sum_{l=1}^N \tilde{\xi}_l(z) \left\langle \frac{\partial u}{\partial \overrightarrow{\mathbf{n}}}(\cdot,\tau), \tilde{\xi}_l(\cdot) \right\rangle_{\kappa,\partial \Omega} \mathrm{d}\tau. \end{split}$$

For $t \in (t_{m_0-1}, t_{m_0}]$ with $1 \le m_0 \le K$, the left side of the above equality can be written as

$$\int_{0}^{t} \int_{\Omega} F(x, t - \tau) w_{z}^{N}(x, \tau) dx d\tau = \int_{0}^{t - t_{m_{0} - 1}} \int_{\Omega} p_{m_{0}}(x) w_{z}^{N}(x, \tau) dx d\tau + \sum_{m=1}^{m_{0} - 1} \int_{t - t_{m}}^{t - t_{m-1}} \int_{\Omega} p_{m}(x) w_{z}^{N}(x, \tau) dx d\tau.$$

Similarly, if $t > t_K$, we have

$$\int_0^t \int_{\Omega} F(x, t - \tau) w_z^N(x, \tau) dx d\tau = \sum_{m=1}^K \int_{t-t_m}^{t-t_{m-1}} \int_{\Omega} p_m(x) w_z^N(x, \tau) dx d\tau.$$

Then for the above equality, differentiating at time t gives that for $t \in (t_{m_0-1}, t_{m_0}]$ with $1 \le m_0 \le K$,

$$\begin{split} -\sum_{l=1}^{N} \tilde{\xi}_{l}(z) \left\langle \frac{\partial u}{\partial \overrightarrow{\mathbf{n}}}(\cdot, t), \tilde{\xi}_{l}(\cdot) \right\rangle_{\kappa, \partial \Omega} &= \int_{\Omega} p_{m_{0}}(x) w_{z}^{N}(x, t - t_{m_{0}-1}) \mathrm{d}x \\ &+ \sum_{m=1}^{m_{0}-1} \int_{\Omega} p_{m}(x) \left[w_{z}^{N}(x, t - t_{m-1}) - w_{z}^{N}(x, t - t_{m}) \right] \mathrm{d}x, \end{split}$$

and for $t > t_K$ (from assumption 1.2, we see that K is finite),

$$-\sum_{l=1}^{N} \tilde{\xi}_{l}(z) \left\langle \frac{\partial u}{\partial \overrightarrow{\mathbf{n}}}(\cdot,t), \tilde{\xi}_{l}(\cdot) \right\rangle_{\kappa,\partial\Omega} = \sum_{m=1}^{K} \int_{\Omega} p_{m}(x) \left[w_{z}^{N}(x,t-t_{m-1}) - w_{z}^{N}(x,t-t_{m}) \right] dx.$$

From assumption 2.4(c) we have for a.e. $t > t_K$,

$$-\frac{\partial u}{\partial \overrightarrow{\mathbf{n}}}(z,t) = \sum_{m=1}^{K} \lim_{N \to \infty} \int_{\Omega} p_m(x) \left[w_z^N(x,t-t_{m-1}) - w_z^N(x,t-t_m) \right] dx,$$

and for a.e. $t \in (t_{m_0-1}, t_{m_0}]$ with $1 \le m_0 \le K$,

$$-\frac{\partial u}{\partial \overrightarrow{\mathbf{n}}}(z,t) = \lim_{N \to \infty} \int_{\Omega} p_{m_0}(x) w_z^N(x,t-t_{m_0-1}) dx$$

$$+ \sum_{m=1}^{m_0-1} \lim_{N \to \infty} \int_{\Omega} p_m(x) \left[w_z^N(x,t-t_{m-1}) - w_z^N(x,t-t_m) \right] dx.$$

Assumption 1.2(a) ensures that for a fixed t, the summations on the right sides of the above results are finite. Therefore, the order of summation and limit can be exchanged. Moreover, the proof for $t \in [0, t_0]$ is trivial. The proof is complete.

From the above lemma, the following corollary can be deduced.

Corollary 3.2. *For a.e.* $z \in \partial \Omega$ *and* $t \in (0, \infty)$ *, it holds that*

$$-\int_0^t \frac{\partial u}{\partial \overrightarrow{\mathbf{n}}}(z,\tau) d\tau = \int_0^t \sum_{k=1}^K \chi_{t-\tau \in [t_{k-1},t_k)} \left[\sum_{n=1}^\infty c_{z,n} p_{k,n} (1-\mathrm{e}^{-\lambda_n \tau}) \right] d\tau.$$

Here $p_{k,n}$ and $c_{z,n}$ are defined in (2.4).

Proof. Firstly, let us evaluate the limit $\lim_{N\to\infty}\langle p_k(\cdot), \overline{w_z^N(\cdot,t)}\rangle_{\Omega}$ for $k=1,\ldots,K$ and $t\in(0,\infty)$. Fixing $N\in\mathbb{N}^+$, from the definition of ψ_z^N we have $\psi_z^N\in L^2(\Omega)$. So the Fourier expansion of ψ_z^N can be given as $\psi_z^N=\sum_{n=1}^\infty c_{z,n}^N\overline{\varphi_n}$, where $c_{z,n}^N$ is defined in (2.4). Moreover, from $w_z^N=u_z^N+\psi_z^N$ and equation (2.3), we have

$$w_z^N(x,t) = \sum_{n=1}^{\infty} c_{z,n}^N (1 - e^{-\lambda_n t}) \overline{\varphi_n(x)}.$$

The above result together with the regularity $\psi_z^N \in L^2(\Omega)$ yields that $w_z^N(\cdot,t) \in L^2(\Omega)$ for $t \in [0,\infty)$. Also recall that $p_k \in L^2(\Omega)$, then

$$\langle p_k(\cdot), \overline{w_z^N(\cdot, t)} \rangle_{\Omega} = \sum_{r=1}^{\infty} c_{z,n}^N p_{k,n} (1 - e^{-\lambda_n t}).$$

The condition in assumption 2.4 implies that the dominated convergence theorem can be applied to the above series. So we have

$$\lim_{N \to \infty} \sum_{n=1}^{\infty} c_{z,n}^{N} p_{k,n} (1 - e^{-\lambda_n t}) = \sum_{n=1}^{\infty} \lim_{N \to \infty} c_{z,n}^{N} p_{k,n} (1 - e^{-\lambda_n t}).$$

From (2.4), we have

$$\lim_{N\to\infty} \langle p_k(\cdot), \overline{w_z^N(\cdot, t)} \rangle_{\Omega} = \lim_{N\to\infty} \sum_{n=1}^{\infty} c_{z,n}^N p_{k,n} (1 - e^{-\lambda_n t}) = \sum_{n=1}^{\infty} c_{z,n} p_{k,n} (1 - e^{-\lambda_n t}).$$

Now we claim that for t > 0,

$$-\int_0^t \frac{\partial u}{\partial \overrightarrow{\mathbf{n}}}(z,\tau) d\tau = \int_0^t \sum_{k=1}^K \chi_{t-\tau \in [t_{k-1},t_k)} \left[\sum_{n=1}^\infty c_{z,n} p_{k,n} (1 - e^{-\lambda_n \tau}) \right] d\tau.$$
 (3.1)

If $t \leqslant t_0$, from lemma 3.1 we have $\frac{\partial u}{\partial \overline{\mathbf{n}}}(z,\tau) = 0$ for $\tau \leqslant t$. This means (3.1) is valid. For $t \in (t_{m_0-1},t_{m_0}]$ with $1 \leqslant m_0 \leqslant K$, lemma 3.1 yields that

$$-\int_{0}^{t} \frac{\partial u}{\partial \overrightarrow{\mathbf{n}}}(z,\tau) d\tau = -\sum_{m=1}^{m_{0}-1} \int_{t_{m-1}}^{t_{m}} \frac{\partial u}{\partial \overrightarrow{\mathbf{n}}}(z,\tau) d\tau - \int_{t_{m_{0}-1}}^{t} \frac{\partial u}{\partial \overrightarrow{\mathbf{n}}}(z,\tau) d\tau$$

$$= \sum_{m=1}^{m_{0}-1} \int_{t_{m-1}}^{t_{m}} \sum_{l=1}^{m-1} \sum_{n=1}^{\infty} c_{z,n} p_{l,n} (e^{-\lambda_{n}(\tau - t_{l})} - e^{-\lambda_{n}(\tau - t_{l-1})}) d\tau$$

$$+ \sum_{m=1}^{m_{0}-1} \int_{t_{m-1}}^{t_{m}} \sum_{n=1}^{\infty} c_{z,n} p_{m,n} (1 - e^{-\lambda_{n}(\tau - t_{m-1})}) d\tau$$

$$+ \int_{t_{m_{0}-1}}^{t} \sum_{l=1}^{\infty} \sum_{n=1}^{\infty} c_{z,n} p_{l,n} (e^{-\lambda_{n}(\tau - t_{l})} - e^{-\lambda_{n}(\tau - t_{l-1})}) d\tau$$

$$+ \int_{t_{m_{0}-1}}^{t} \sum_{n=1}^{\infty} c_{z,n} p_{m_{0},n} (1 - e^{-\lambda_{n}(\tau - t_{m_{0}-1})}) d\tau$$

$$=: S_{1} + S_{2} + S_{3} + S_{4}.$$

The straightforward computation gives that

$$\begin{split} S_1 &= \sum_{m=1}^{m_0-1} \sum_{l=1}^{m-1} \int_{t_{m-1}-t_{l-1}}^{t_m-t_{l-1}} \sum_{n=1}^{\infty} c_{z,n} p_{l,n} (1-\mathrm{e}^{-\lambda_n \tau}) \mathrm{d}\tau - \sum_{m=1}^{m_0-1} \sum_{l=1}^{m-1} \int_{t_{m-1}-t_{l}}^{t_m-t_{l}} \sum_{n=1}^{\infty} c_{z,n} p_{l,n} (1-\mathrm{e}^{-\lambda_n \tau}) \mathrm{d}\tau \\ &= \sum_{l=1}^{m_0-2} \sum_{m=l+1}^{m_0-1} \int_{t_{m-1}-t_{l-1}}^{t_m-t_{l-1}} \sum_{n=1}^{\infty} c_{z,n} p_{l,n} (1-\mathrm{e}^{-\lambda_n \tau}) \mathrm{d}\tau - \sum_{l=1}^{m_0-2} \sum_{m=l+1}^{m_0-1} \int_{t_{m-1}-t_{l}}^{t_m-t_{l}} \sum_{n=1}^{\infty} c_{z,n} p_{l,n} (1-\mathrm{e}^{-\lambda_n \tau}) \mathrm{d}\tau \\ &= \sum_{l=1}^{m_0-2} \int_{t_{l}-t_{l-1}}^{t_{m_0-1}-t_{l-1}} \sum_{n=1}^{\infty} c_{z,n} p_{l,n} (1-\mathrm{e}^{-\lambda_n \tau}) \mathrm{d}\tau - \sum_{l=1}^{m_0-2} \int_{0}^{t_{m_0-1}-t_{l}} \sum_{n=1}^{\infty} c_{z,n} p_{l,n} (1-\mathrm{e}^{-\lambda_n \tau}) \mathrm{d}\tau. \end{split}$$

Similarly, we have

$$\begin{split} S_2 &= \sum_{m=1}^{m_0-1} \int_0^{t_m-t_{m-1}} \sum_{n=1}^{\infty} c_{z,n} p_{m,n} (1-\mathrm{e}^{-\lambda_n \tau}) \mathrm{d}\tau, \\ S_3 &= \sum_{l=1}^{m_0-1} \int_{t_{m_0-1}-t_{l-1}}^{t-t_{l-1}} \sum_{n=1}^{\infty} c_{z,n} p_{l,n} (1-\mathrm{e}^{-\lambda_n \tau}) \mathrm{d}\tau - \sum_{l=1}^{m_0-1} \int_{t_{m_0-1}-t_l}^{t-t_l} \sum_{n=1}^{\infty} c_{z,n} p_{l,n} (1-\mathrm{e}^{-\lambda_n \tau}) \mathrm{d}\tau, \\ S_4 &= \int_0^{t-t_{m_0-1}} \sum_{n=1}^{\infty} c_{z,n} p_{m_0,n} (1-\mathrm{e}^{-\lambda_n \tau}) \mathrm{d}\tau = \int_0^t \chi_{t-\tau \in [t_{m_0-1},t_{m_0})} \sum_{n=1}^{\infty} c_{z,n} p_{m_0,n} (1-\mathrm{e}^{-\lambda_n \tau}) \mathrm{d}\tau. \end{split}$$

These give that

$$\begin{split} S_1 + S_2 + S_3 &= \sum_{l=1}^{m_0 - 2} \int_0^{t - t_{l-1}} \sum_{n=1}^{\infty} c_{z,n} p_{l,n} (1 - \mathrm{e}^{-\lambda_n \tau}) \mathrm{d}\tau - \sum_{l=1}^{m_0 - 2} \int_0^{t - t_l} \sum_{n=1}^{\infty} c_{z,n} p_{l,n} (1 - \mathrm{e}^{-\lambda_n \tau}) \mathrm{d}\tau \\ &+ \int_0^{t - t_{m_0 - 2}} \sum_{n=1}^{\infty} c_{z,n} p_{m_0 - 1,n} (1 - \mathrm{e}^{-\lambda_n \tau}) \mathrm{d}\tau - \int_0^{t - t_{m_0 - 1}} \sum_{n=1}^{\infty} c_{z,n} p_{m_0 - 1,n} (1 - \mathrm{e}^{-\lambda_n \tau}) \mathrm{d}\tau \\ &= \sum_{l=1}^{m_0 - 1} \int_{t - t_l}^{t - t_{l-1}} \sum_{n=1}^{\infty} c_{z,n} p_{l,n} (1 - \mathrm{e}^{-\lambda_n \tau}) \mathrm{d}\tau \\ &= \int_0^{t} \sum_{l=1}^{m_0 - 1} \chi_{t - \tau \in [t_{l-1}, t_l)} \left[\sum_{n=1}^{\infty} c_{z,n} p_{l,n} (1 - \mathrm{e}^{-\lambda_n \tau}) \right] \mathrm{d}\tau. \end{split}$$

Hence, it holds that

$$-\int_0^t \frac{\partial u}{\partial \overrightarrow{\mathbf{n}}}(z,\tau) d\tau = S_1 + S_2 + S_3 + S_4$$

$$= \int_0^t \sum_{l=1}^{m_0} \chi_{t-\tau \in [t_{l-1},t_l)} \left[\sum_{n=1}^{\infty} c_{z,n} p_{l,n} (1 - e^{-\lambda_n \tau}) \right] d\tau,$$

which confirms the claim.

When *K* is finite, we can pick t > 0 such that $t > t_K$. In this case, the term S_4 is eliminated, and $m_0 - 1$ is replaced by *K* in the terms S_1, S_2, S_3 . So the claim (3.1) is still valid.

Above all, we have proved the claim (3.1) and the proof is complete.

3.2. The analysis of Laplace transform

The proof of theorem 1 will rely on the Laplace transform \mathcal{L} , defined as

$$\mathcal{L}\{\psi(t)\}(s) = \int_0^\infty e^{-st} \psi(t) dt, \quad s \in \mathbb{C}.$$

Recalling the result in corollary 3.2, it is not hard to see that

$$\mathcal{L}\{1 - e^{-\lambda_n t}\}(s) = \lambda_n s^{-1} (s + \lambda_n)^{-1}, \text{ Re } s > 0.$$

Also, assumption 2.4 gives that

$$\left| \int_{0}^{t} \sum_{k=1}^{K} \chi_{t-\tau \in [t_{k-1},t_k)} \left[\sum_{n=1}^{\infty} c_{z,n} p_{k,n} (1 - e^{-\lambda_n \tau}) \right] d\tau \right| \leqslant 2t \sum_{k=1}^{K} \sum_{n=1}^{\infty} |c_{z,n} p_{k,n}|$$

$$\leqslant Ct,$$

and we have $|e^{-st}t|$ is integrable on $(0,\infty)$ for Re s>0. This means that the dominated convergence theorem can be used and it gives that for $\operatorname{Re} s > 0$,

$$\mathcal{L}\left\{-\int_{0}^{t} \frac{\partial u}{\partial \overrightarrow{\mathbf{n}}}(z,\tau) d\tau\right\}(s) = \sum_{k=1}^{K} \int_{0}^{\infty} e^{-st} \int_{0}^{t} \chi_{t-\tau \in [t_{k-1},t_{k})} \left[\sum_{n=1}^{\infty} c_{z,n} p_{k,n} (1 - e^{-\lambda_{n}\tau})\right] d\tau dt$$

$$= \sum_{k=1}^{K} \left[\int_{0}^{\infty} e^{-st} \chi_{t \in [t_{k-1},t_{k})} dt\right] \left[\int_{0}^{\infty} e^{-st} \sum_{n=1}^{\infty} c_{z,n} p_{k,n} (1 - e^{-\lambda_{n}t}) dt\right]$$

$$= \sum_{k=1}^{K} s^{-2} (e^{-t_{k-1}s} - e^{-t_{k}s}) \left[\sum_{n=1}^{\infty} c_{z,n} p_{k,n} \lambda_{n} (s + \lambda_{n})^{-1}\right].$$

Hence, we see that for Re s > 0,

$$s^{2}\mathcal{L}\left\{-\int_{0}^{t} \frac{\partial u}{\partial \overrightarrow{\mathbf{n}}}(z,\tau) d\tau\right\}(s) = \sum_{k=1}^{K} \left(e^{-t_{k-1}s} - e^{-t_{k}s}\right) \left[\sum_{n=1}^{\infty} c_{z,n} p_{k,n} \lambda_{n} (s+\lambda_{n})^{-1}\right]. \tag{3.2}$$

We index the set of distinct eigenvalues as $\{\lambda_i\}_{i=1}^{\infty}$ with increasing order. Then we give the next lemma, which contains the well-definedness and the analyticity of the above complexvalued series.

Lemma 3.3. *Under assumption* 2.4, *we have the following properties:*

- (a) For R > 0 we define $\Lambda_R := \{s \in \mathbb{C} : |s| < R\}$, then for each $k \in \{1, ..., K\}$, $\sum_{n=1}^{\infty} c_{z,n} p_{k,n} \lambda_n (s + \lambda_n)^{-1} \text{ is uniformly convergent for } s \in \Lambda_R \setminus \{-\lambda_j\}_{j=1}^{\infty};$ (b) $\sum_{n=1}^{\infty} c_{z,n} p_{k,n} \lambda_n (s + \lambda_n)^{-1} \text{ is holomorphic on } \mathbb{C} \setminus \{-\lambda_j\}_{j=1}^{\infty};$ (c) The series $\sum_{k=1}^{K} (e^{-t_{k-1}s} e^{-t_ks}) \left[\sum_{n=1}^{\infty} c_{z,n} p_{k,n} \lambda_n (s + \lambda_n)^{-1}\right] \text{ is analytic on } \mathbb{C}^+ := \{s \in \mathbb{C} : \text{Re } s > 0\}.$

Proof. For (a), fixing R > 0, since $\lim_{n \to \infty} \lambda_n = \infty$, then we can find large enough $N_1 \in \mathbb{N}^+$ such that $\lambda_n \ge 2R$ if $n > N_1$. For $s \in \Lambda_R \setminus \{-\lambda_i\}_{i=1}^{\infty}$ and $n > N_1$,

$$|s + \lambda_n| \geqslant |\operatorname{Re} s + \lambda_n| = \operatorname{Re} s + \lambda_n \geqslant \lambda_n - R.$$

This means that $|\lambda_n(s+\lambda_n)^{-1}| \leq 2$. Given $\epsilon > 0$, from assumption 2.4, we can find $N_2 > 0$ such that $\sum_{n=n_0}^{\infty} |c_{z,n}p_{k,n}| < \epsilon/2$ if $n_0 > N_2$. Hence, for $n_0 > \max\{N_1, N_2\}$, we have

$$\left| \sum_{n=n_0}^{\infty} c_{z,n} p_{k,n} \lambda_n (s+\lambda_n)^{-1} \right| \leq 2 \sum_{n=n_0}^{\infty} |c_{z,n} p_{k,n}| < \epsilon \quad \text{for } s \in \Lambda_R \setminus \{-\lambda_j\}_{j=1}^{\infty}.$$

This gives the uniform convergence.

For (b), fixing R > 0, it is clear that $c_{z,n}p_{k,n}\lambda_n(s+\lambda_n)^{-1}$ is holomorphic on $\Lambda_R\setminus\{-\lambda_j\}_{j=1}^{\infty}$. Then the uniform convergence gives that $\sum_{n=1}^{\infty} c_{z,n} p_{k,n} \lambda_n (s+\lambda_n)^{-1}$ is holomorphic on $\Lambda_R \setminus \{-\lambda_j\}_{j=1}^{\infty}$. For each $s_0 \in \mathbb{C} \setminus \{-\lambda_j\}_{j=1}^{\infty}$, we can find a sufficiently large R > 0 such that $s_0 \in \mathbb{C} \setminus \{-\lambda_j\}_{j=1}^{\infty}$ $\Lambda_R \setminus \{-\lambda_j\}_{j=1}^{\infty}$. This means that $\sum_{n=1}^{\infty} c_{z,n} p_{k,n} \lambda_n (s+\lambda_n)^{-1}$ is holomorphic on $s=s_0$, which leads to the desired result.

For (c), for $s \in \mathbb{C}^+$, we have $|e^{-t_{k-1}s} - e^{-t_ks}| \le 2$ and $|\lambda_n(s + \lambda_n)^{-1}| \le 1$. Also, assumption 2.4 gives that $\sum_{k=1}^K \sum_{n=1}^\infty |c_{z,n}p_{k,n}| < \infty$, then following the proof for (a), we obtain that the series

$$\sum_{k=1}^{K} (e^{-t_{k-1}s} - e^{-t_k s}) \left[\sum_{n=1}^{\infty} c_{z,n} p_{k,n} \lambda_n (s + \lambda_n)^{-1} \right]$$

is uniformly convergent on \mathbb{C}^+ . Sequentially, from the proof for (b), the holomorphic result can be derived, and the proof is complete.

3.3. Some auxiliary lemmas

Before showing theorem 1, we list and prove several auxiliary lemmas.

Lemma 3.4. Recall that $\{\lambda_j\}_{j=1}^{\infty}$ is the set of distinct eigenvalues with increasing order. For any nonempty open subset $\Gamma \subset \partial \Omega$, if

$$\sum_{\lambda_n = \lambda_j} c_{z,n} \eta_n = 0 \quad \text{for } j \in \mathbb{N}^+ \quad \text{and a.e. } z \in \Gamma,$$

then $\{\eta_n\}_{n=1}^{\infty} = \{0\}.$

Proof. Fixing $j \in \mathbb{N}^+$, from the proof of lemma 2.4, we have

$$\begin{split} c_{z,n} &= \lambda_j^{-1} \lim_{N \to \infty} \langle \psi_z^N, \mathcal{A} \overline{\varphi_n} \rangle_{\Omega} \\ &= \lambda_j^{-1} \lim_{N \to \infty} \left(\langle \mathcal{A} \psi_z^N, \overline{\varphi_n} \rangle_{\Omega} - \langle \psi_z^N, \frac{\partial \overline{\varphi_n}}{\partial \overrightarrow{\mathbf{n}}} \rangle_{\kappa, \partial \Omega} + \langle \frac{\partial \psi_z^N}{\partial \overrightarrow{\mathbf{n}}}, \overline{\varphi_n} \rangle_{\kappa, \partial \Omega} \right) \\ &= -\lambda_j^{-1} \sum_{l=1}^{\infty} \tilde{\xi}_l(z) \langle \frac{\partial \varphi_n}{\partial \overrightarrow{\mathbf{n}}}, \tilde{\xi}_l \rangle_{\kappa, \partial \Omega}. \end{split}$$

With the definition of the orthonormal basis $\{\tilde{\xi}_l\}_{l=1}^{\infty}$, the above series is actually finite. This gives that for a.e. $z \in \Gamma$,

$$\sum_{l=1}^{\infty} \tilde{\xi}_l(z) \langle \frac{\partial \varphi_n}{\partial \overrightarrow{\mathbf{n}}}, \tilde{\xi}_l \rangle_{\kappa, \partial \Omega} = \frac{\partial \varphi_n}{\partial \overrightarrow{\mathbf{n}}}(z),$$

which leads to $\sum_{\lambda_n=\lambda_j} \eta_n \frac{\partial \varphi_n}{\partial \mathbf{n}}(z) = 0$ for a.e. $z \in \Gamma$. Assume that $\{\eta_n : \lambda_n = \lambda_j\} \neq \{0\}$, then the linear independence of the set $\{\varphi_n(x) : \lambda_n = \lambda_j\}$ yields that $\sum_{\lambda_n=\lambda_j} \eta_n \varphi_n(x)$ is not vanishing on Ω . However, we see that $\sum_{\lambda_n=\lambda_j} \eta_n \varphi_n(x)$ is an eigenfunction corresponding to the eigenvalue λ_j . These and lemma 2.1 give that $\sum_{\lambda_n=\lambda_j} \eta_n \frac{\partial \varphi_n}{\partial \mathbf{n}}$ cannot vanish almost everywhere on Γ , which is a contradiction. Hence, we prove that $\{\eta_n : \lambda_n = \lambda_j\} = \{0\}$ for each $j \in \mathbb{N}^+$, namely, $\eta_n = 0$ for $n \in \mathbb{N}^+$. The proof is complete.

Lemma 3.5. Set $\Gamma \subset \partial \Omega$ to be a nonempty open subset and let $\sum_{n=1}^{\infty} c_{z,n} \eta_n$ be absolute convergent for a.e. $z \in \Gamma$. Then given $\epsilon > 0$, the result

$$\sum_{n=1}^{\infty} c_{z,n} \eta_n (1 - e^{-\lambda_n t}) = 0 \quad \text{for } t \in (0, \epsilon) \quad \text{and a.e. } z \in \Gamma$$

implies that $\eta_n = 0$ for $n \in \mathbb{N}^+$.

Proof. From [23, lemma 3.5] we have that $\sum_{\lambda_n=\lambda_j} c_{z,n} \eta_n = 0$ for each $j \in \mathbb{N}^+$ and a.e. $z \in \Gamma$. Then lemma 3.4 gives the desired result and completes the proof.

Lemma 3.6. Let the conditions in lemma 3.5 be valid. For $s \in \mathbb{C}^+$, if $\exists \epsilon > 0$ such that

$$\lim_{\mathrm{Re} s \to \infty} \mathrm{e}^{\epsilon s} \left[\sum_{n=1}^{\infty} c_{z,n} \lambda_n \eta_n (s + \lambda_n)^{-1} \right] = 0 \quad \text{for a.e. } z \in \Gamma,$$

then $\{\eta_n\}_{n=1}^{\infty} = \{0\}.$

Proof. For a.e. $z \in \Gamma$, we define

$$F_z(t) := \chi_{t \geqslant 0} \sum_{n=-1}^{\infty} c_{z,n} \eta_n (1 - e^{-\lambda_n t}), \quad t \in (-\infty, \infty).$$

From the absolute convergence of the series $\sum_{n=1}^{\infty} c_{z,n} \eta_n$, we see that

$$|F_z(t)| \leqslant C \sum_{n=1}^{\infty} |c_{z,n}\eta_n| \leqslant C < \infty.$$

Also, the direct computation yields that

$$\int_{-\epsilon}^{\infty} |e^{-st}| \int_{0}^{t+\epsilon} |F_{z}(\tau)| d\tau dt \leqslant C \int_{-\epsilon}^{\infty} e^{-tRes} (t+\epsilon) dt$$

$$= C e^{\epsilon Res} \int_{0}^{\infty} e^{-tRes} t dt$$

$$= C e^{\epsilon Res} (Re s)^{-2} < \infty.$$

This implies the well-definedness of the integration $\int_{-\epsilon}^{\infty} |e^{-st}| \int_{0}^{t+\epsilon} |F_z(\tau)| d\tau dt$ for Re s > 0 and a.e. $z \in \Gamma$.

Introducing the Heaviside function $H(t) := \chi_{t \ge 0}$, we see that

$$\int_{-\epsilon}^{\infty} e^{-st} \int_{0}^{t+\epsilon} F_{z}(\tau) d\tau dt = \int_{-\infty}^{\infty} e^{-st} \int_{-\infty}^{\infty} H(t-\tau+\epsilon) F_{z}(\tau) d\tau dt.$$

The above argument provides the well-definedness of the integral

$$\int_{-\infty}^{\infty} e^{-st} \int_{-\infty}^{\infty} H(t-\tau+\epsilon) F_{z}(\tau) d\tau dt$$

when Re s > 0. With Fubini theorem and the dominated convergence theorem, we have,

$$\int_{-\infty}^{\infty} e^{-ts} \int_{-\infty}^{\infty} H(t - \tau + \epsilon) F_z(\tau) d\tau dt$$

$$= \int_{-\epsilon}^{\infty} e^{-ts} dt \int_{0}^{\infty} e^{-\tau s} \left[\sum_{n=1}^{\infty} c_{z,n} \eta_n (1 - e^{-\lambda_n \tau}) \right] d\tau$$

$$= s^{-2} e^{\epsilon s} \left[\sum_{n=1}^{\infty} c_{z,n} \lambda_n \eta_n (s + \lambda_n)^{-1} \right], \quad \text{Re } s > 0,$$

which leads to

$$\lim_{\mathrm{Re} s \to \infty} \int_{-\infty}^{\infty} \mathrm{e}^{-ts} \int_{-\infty}^{\infty} H(t - \tau + \epsilon) F_z(\tau) \mathrm{d}\tau \, \mathrm{d}t = 0.$$

Also, from the direct calculation, we have

$$\begin{split} \int_{-\infty}^{\infty} \mathrm{e}^{-ts} \int_{-\infty}^{\infty} & H(t-\tau+\epsilon) F_z(\tau) \mathrm{d}\tau \, \mathrm{d}t = \int_{-\epsilon}^{\infty} \mathrm{e}^{-ts} \left[\sum_{n=1}^{\infty} c_{z,n} \int_{0}^{t+\epsilon} \eta_n (1-\mathrm{e}^{-\lambda_n \tau}) \mathrm{d}\tau \right] \mathrm{d}t \\ &= \int_{0}^{\epsilon} \mathrm{e}^{(\epsilon-t)s} \left[\sum_{n=1}^{\infty} c_{z,n} \int_{0}^{t} \eta_n (1-\mathrm{e}^{-\lambda_n \tau}) \mathrm{d}\tau \right] \mathrm{d}t \\ &+ \int_{0}^{\infty} \mathrm{e}^{-ts} \left[\sum_{n=1}^{\infty} c_{z,n} \int_{0}^{t+\epsilon} \eta_n (1-\mathrm{e}^{-\lambda_n \tau}) \mathrm{d}\tau \right] \mathrm{d}t \\ &=: S_{z,1}(s) + S_{z,2}(s). \end{split}$$

For $S_{z,2}(s)$, the dominated convergence theorem and the absolute convergence of $\sum_{n=1}^{\infty} c_{z,n} \eta_n$ give that

$$|S_{z,2}(s)| \leqslant C \sum_{n=1}^{\infty} |c_{z,n}\eta_n| \int_0^{\infty} e^{-tRes} |t + \epsilon| dt,$$

and clearly the right side converges to 0 as Re $s \to \infty$. So $\lim_{\text{Re}s \to \infty} S_{z,2}(s) = 0$. With the limit assumption in this lemma, we have

$$\lim_{\text{Res} \to \infty} S_{z,1}(s) = \lim_{\text{Res} \to \infty} [S_{z,1}(s) + S_{z,2}(s)] - \lim_{\text{Res} \to \infty} S_{z,2}(s) = 0.$$

For each $R_0 \in \mathbb{R}$, when Re $s \in (-\infty, R_0)$, we can see

$$|S_{z,1}(s)| \leqslant C \int_0^{\epsilon} e^{(\epsilon - t) \operatorname{Res} t} \sum_{n=1}^{\infty} |c_{z,n} \eta_n| dt \leqslant C e^{\epsilon R_0} \int_0^{\epsilon} t dt = C_{\epsilon,R_0} < \infty.$$

This with the limit result $\lim_{\mathrm{Re}s\to\infty} S_{z,1}(s)=0$ yields that $S_{z,1}(s)$ is well-defined and bounded on the whole complex plane $\mathbb C$. The definition of $S_{z,1}(s)$ gives that $S_{z,1}(s)$ is holomorphic on $\mathbb C$. Hence, we have that $S_{z,1}(s)$ is a bounded entire function for a.e. $z\in\Gamma$, which with Liouville's theorem yields that $S_{z,1}\equiv C$ on $\mathbb C$. Considering the limit result $\lim_{\mathrm{Re}s\to\infty} S_{z,1}(s)=0$, it gives that

$$S_{z,1}(s) = 0$$
 for $s \in \mathbb{C}$ and a.e. $z \in \Gamma$.

Then we can see

$$S_{z,1}(s) = \int_0^{\epsilon} e^{(\epsilon - t)s} \left[\sum_{n=1}^{\infty} c_{z,n} \int_0^t \eta_n (1 - e^{-\lambda_n \tau}) d\tau \right] dt$$
$$= e^{\epsilon s} \int_0^{\epsilon} e^{-ts} \left[\sum_{n=1}^{\infty} c_{z,n} \int_0^t \eta_n (1 - e^{-\lambda_n \tau}) d\tau \right] dt \equiv 0,$$

which means for Re s > 0,

$$0 \equiv \int_0^\infty e^{-st} H(\epsilon - t) \left[\sum_{n=1}^\infty c_{z,n} \int_0^t \eta_n (1 - e^{-\lambda_n \tau}) d\tau \right] dt$$
$$= \mathcal{L} \left\{ H(\epsilon - t) \sum_{n=1}^\infty c_{z,n} \int_0^t \eta_n (1 - e^{-\lambda_n \tau}) d\tau \right\} (s).$$

Using [11, corollary 8.1], it follows that

$$\sum_{n=1}^{\infty} c_{z,n} \int_0^t \eta_n (1 - \mathrm{e}^{-\lambda_n \tau}) \mathrm{d}\tau = 0, \quad t \in (0,\epsilon).$$

The absolute convergence of $\sum_{n=1}^{\infty} c_{z,n} \eta_n$ supports the uniform convergence of

$$\sum_{n=1}^{\infty} c_{z,n} \int_0^t \eta_n (1 - e^{-\lambda_n \tau}) d\tau \quad \text{and} \quad \sum_{n=1}^{\infty} c_{z,n} \eta_n (1 - e^{-\lambda_n t})$$

on $(0, \epsilon)$. Thus, from [21, theorem 7.17], differentiating the series $\sum_{n=1}^{\infty} c_{z,n} \int_{0}^{t} \eta_{n} (1 - e^{-\lambda_{n}\tau}) d\tau$ on t yields that for $t \in (0, \epsilon)$ and a.e. $z \in \Gamma$,

$$0 = \frac{\mathrm{d}}{\mathrm{d}t} \left[\sum_{n=1}^{\infty} c_{z,n} \int_0^t \eta_n (1 - \mathrm{e}^{-\lambda_n \tau}) \mathrm{d}\tau \right] = \sum_{n=1}^{\infty} c_{z,n} \eta_n (1 - \mathrm{e}^{-\lambda_n t}).$$

This together with lemma 3.5 leads to $\eta_n = 0$ for $n \in \mathbb{N}^+$, and completes the proof.

3.4. Proof of theorem 1

Now, it is time to show theorem 1. For shorten the proof, the following notations will be used:

$$p_{k,n} = \langle p_k(\cdot), \varphi_n(\cdot) \rangle_{\Omega}, \quad Q_{z,k}(s) = \sum_{n=1}^{\infty} c_{z,n} p_{k,n} \lambda_n (s + \lambda_n)^{-1},$$

$$\tilde{p}_{k,n} = \langle \tilde{p}_k(\cdot), \varphi_n(\cdot) \rangle_{\Omega}, \quad \tilde{Q}_{z,k}(s) = \sum_{n=1}^{\infty} c_{z,n} \tilde{p}_{k,n} \lambda_n (s + \lambda_n)^{-1}.$$

Proof of theorem 1. The result (3.2), lemma 3.3 and the analytic continuation give that for $s \in \mathbb{C}^+$ and a.e. $z \in \Gamma$,

$$\sum_{k=1}^{K} (e^{-t_{k-1}s} - e^{-t_k s}) Q_{z,k}(s) = \sum_{k=1}^{K} (e^{-\tilde{t}_{k-1}s} - e^{-\tilde{t}_k s}) \tilde{Q}_{z,k}(s).$$
(3.3)

Firstly, let us show $t_0 = \tilde{t}_0$. Without loss of generality, we can assume that $t_0 < \tilde{t}_0$. Picking $\epsilon > 0$ such that $\epsilon < \min\{\tilde{t}_0 - t_0, t_1 - t_0\}$, from (3.3), we have for $s \in \mathbb{C}^+$ and a.e. $z \in \Gamma$,

$$e^{\epsilon s} Q_{z,1}(s) = e^{(\epsilon + t_0 - t_1)s} Q_{z,1}(s) - \sum_{k=2}^{K} (e^{(\epsilon + t_0 - t_{k-1})s} - e^{(\epsilon + t_0 - t_k)s}) Q_{z,k}(s)$$

$$+ \sum_{k=1}^{\tilde{K}} (e^{(\epsilon + t_0 - \tilde{t}_{k-1})s} - e^{(\epsilon + t_0 - \tilde{t}_k)s}) \tilde{Q}_{z,k}(s).$$
(3.4)

We see that $\lambda_n(s+\lambda_n)^{-1}$ is uniformly bounded on \mathbb{C}^+ . Recalling the convergence result $\sum_{k=1}^K \sum_{n=1}^\infty |c_{z,n}p_{k,n}| < \infty$ from assumption 2.4, the uniform convergence of the series $\sum_{k=2}^K (e^{(\epsilon+t_0-t_{k-1})s} - e^{(\epsilon+t_0-t_k)s})Q_{z,k}(s)$ on the half plane \mathbb{C}^+ can be derived. Then we have,

$$\lim_{\text{Re}s \to \infty} \sum_{k=2}^{K} (e^{(\epsilon + t_0 - t_{k-1})s} - e^{(\epsilon + t_0 - t_k)s}) Q_{z,k}(s) = \sum_{k=2}^{K} \lim_{\text{Re}s \to \infty} (e^{(\epsilon + t_0 - t_{k-1})s} - e^{(\epsilon + t_0 - t_k)s}) Q_{z,k}(s) = 0.$$

Similarly, we see that other terms on the right side of (3.4) also tend to zero as $\operatorname{Re} s \to \infty$. So we have $\lim_{\operatorname{Re} s \to \infty} \operatorname{e}^{\epsilon s} Q_{z,1}(s) = 0$ for a.e. $z \in \Gamma$. This with lemma 3.6 gives that $p_{1,n} = 0$ for $n \in \mathbb{N}^+$, i.e. $\|p_1\|_{L^2(\Omega)} = 0$, which contradicts with assumption 1.2. Hence, we have $t_0 = \tilde{t}_0$. Inserting $t_0 = \tilde{t}_0$ into (3.3) and picking $0 < \epsilon < \min\{t_1 - t_0, \tilde{t}_1 - t_0\}$, we have

$$e^{\epsilon s}[Q_{z,1}(s) - \tilde{Q}_{z,1}(s)] = e^{(\epsilon + t_0 - t_1)s} Q_{z,1}(s) - e^{(\epsilon + t_0 - \tilde{t}_1)s} \tilde{Q}_{z,1}(s)$$

$$- \sum_{k=2}^{K} (e^{(\epsilon + t_0 - t_{k-1})s} - e^{(\epsilon + t_0 - t_k)s}) Q_{z,k}(s)$$

$$+ \sum_{k=2}^{\tilde{K}} (e^{(\epsilon + t_0 - \tilde{t}_{k-1})s} - e^{(\epsilon + t_0 - \tilde{t}_k)s}) \tilde{Q}_{z,k}(s).$$

From the previous arguments, we can prove

$$\lim_{\mathsf{Res}\to\infty} e^{\epsilon s}[Q_{z,1}(s)-\tilde{Q}_{z,1}(s)]=0, \quad \text{a.e. } z\in\Gamma.$$

Lemma 3.6 gives that $p_{1,n} = \tilde{p}_{1,n}$ for $n \in \mathbb{N}^+$, namely $||p_1 - \tilde{p}_1||_{L^2(\Omega)} = 0$.

Next we want to show $t_1 = \tilde{t}_1$. Owing to the results $p_{1,n} = \tilde{p}_{1,n}$ and $t_0 = \tilde{t}_0$ into (3.3), it follows that for $s \in \mathbb{C}^+$ and a.e. $z \in \Gamma$,

$$\begin{aligned} \mathbf{e}^{-t_1s}[Q_{z,2}(s) - Q_{z,1}(s)] &= \mathbf{e}^{-\tilde{t}_1s}[\tilde{Q}_{z,2}(s) - \tilde{Q}_{z,1}(s)] + \mathbf{e}^{-t_2s}Q_{z,2}(s) - \mathbf{e}^{-\tilde{t}_2s}\tilde{Q}_{z,2}(s) \\ &- \sum_{k=3}^{K} (\mathbf{e}^{-t_{k-1}s} - \mathbf{e}^{-t_ks})Q_{z,k}(s) + \sum_{k=3}^{\tilde{K}} (\mathbf{e}^{-\tilde{t}_{k-1}s} - \mathbf{e}^{-\tilde{t}_ks})\tilde{Q}_{z,k}(s). \end{aligned}$$

Without loss of generality, we assume that $t_1 < \tilde{t}_1$ and pick $0 < \epsilon < \min\{\tilde{t}_1 - t_1, t_2 - t_1, \tilde{t}_2 - t_1\}$. Following the proof for $t_0 = \tilde{t}_0$, we can show that $||p_2 - p_1||_{L^2(\Omega)} = 0$. This is a contradiction. Hence $t_1 = \tilde{t}_1$.

Now with the results $t_0 = \tilde{t}_0$, $t_1 = \tilde{t}_1$ and $||p_1 - \tilde{p}_1||_{L^2(\Omega)} = 0$, from (3.3), we have that for Re s > 0 and a.e. $z \in \Gamma$,

$$\sum_{k=2}^{K} (e^{-t_{k-1}s} - e^{-t_k s}) Q_{z,k}(s) = \sum_{k=2}^{\tilde{K}} (e^{-\tilde{t}_{k-1}s} - e^{-\tilde{t}_k s}) \tilde{Q}_{z,k}(s).$$

From the previous proof, we can derive that $t_2 = \tilde{t}_2$ and $||p_2 - \tilde{p}_2||_{L^2(\Omega)} = 0$. Using this technique recursively, we can conclude that

$$t_0 = \tilde{t}_0, \qquad t_k = \tilde{t}_k, \qquad \|p_k - \tilde{p}_k\|_{L^2(\Omega)} = 0 \quad \text{for } k = 1, \dots, \min\{K, \tilde{K}\}.$$
 (3.5)

Finally, we need to show $K = \tilde{K}$. (For the case of $K = \infty$ and $\tilde{K} = \infty$, we regard them as $K = \tilde{K}$.) Without loss of generality assuming that $K < \tilde{K}$, from (3.3) and (3.5), we have for Re S > 0 and a.e. S = C = 0.

$$\sum_{k=K+1}^{\tilde{K}} (e^{-\tilde{t}_{k-1}s} - e^{-\tilde{t}_k s}) \tilde{Q}_{z,k}(s) = 0.$$

The former proof gives that $\|\tilde{p}_{K+1}\|_{L^2(\Omega)} = 0$, which is a contradiction. Hence, we have that $K = \tilde{K}$, which together with (3.5) leads to the desired result. The proof is complete.

4. Numerical reconstructions

In this section, we are going to conduct several numerical experiments which realize the inversion process described in theorem 1. The experiments focus on the recovery of the support of the unknown source. Such experiments are common in some practical applications, such as medical imaging, pollution control, and so on. As we mentioned in section 1, we formulate this inverse source problem as estimating the state of the system (position of the source) when a sequence of observations in time becomes available. The popular choice to solve the sequential prediction problem is the sequential Monte Carlo (SMC) method, which is also called the PF. In this work, we are going to use one variant of the SMC as the approach to solving the inverse problem. Before presenting the results of the numerical experiments, we will first review some preliminaries of the SMC algorithm.

4.1. Sequential Monte Carlo (SMC)

Consider a discrete-time Markov process $\{x_t\}_{t=0}^n$:

$$x_0 \sim p(x_0)$$
 and $x_n | x_{n-1} \sim p(x_n | x_{n-1}),$ (4.1)

where \sim means distributed as, $p(x_0)$ is the prior of the initial state x_0 and p(x'|x) is the given transition probability prior from current state x to the next state x'. We are interested in estimating $\{x_t\}_{t=0}^n$ which is also denoted as $x_{0:n}$, given the observations $\{y_t\}_{t=0}^n$ at each time step. The state x_t is the position of the support of the source and y_t is the flux on the boundary.

The equation (4.1) together with the likelihood $p(y_t|x_t)$ will define a Bayesian model. We have the prior on the trajectory $x_{0:n} := \{x_0, \dots, x_n\}$ as follows:

$$p(x_{0:n}) = p(x_0) \prod_{k=1}^{n} p(x_k | x_{k-1}).$$
(4.2)

Moreover,

$$p(y_{0:n}|x_{0:n}) = \prod_{k=1}^{n} p(y_k|x_k). \tag{4.3}$$

From a Bayesian perspective, the posterior distribution of $x_{0:n}$ given a sequence of the observations $y_{0:n}$ is:

$$p(x_{0:n}|y_{0:n}) = \frac{p(x_{0:n}, y_{0:n})}{p(y_{0:n})},$$
(4.4)

where $p(x_{0:n}, y_{0:n}) = p(y_{0:n}|x_{0:n})p(x_{0:n})$ and $p(y_{0:n}) = \int p(x_{0:n}, y_{0:n}) dx_{0:n}$.

In our application, the most time-consuming step is to evaluate the likelihood function $p(y_{0:n}|x_{0:n})$, and we will follow the classical framework as in [24]. Denoting the forward solver, which maps the input state u to the observation y as \mathcal{G} , it follows that

$$y = \mathcal{G}(u) + \eta$$

where η is the error associated with the process. There are various sources of error. For example, the error in the observation and the error of the forward solver. The total error η is then assumed to follow the Gaussian distribution, $\mathcal{N}(0,B)$ where B is the covariance with a proper size. The likelihood function then has the form:

$$p(y|u) := p(y - \mathcal{G}(u)) = p(\eta) \sim \mathcal{N}(0, B).$$

Now the area of interest is the tracking problem: find the current state given the observations. Theoretically, this means that one needs to find a group of $p(x_{0:n}|y_{0:n})$. By the prior (4.2) and the likelihood (4.3), the joint distribution $p(x_{0:n}, y_{0:n})$ in (4.4) then satisfies

$$p(x_{0:n}, y_{0:n}) = p(x_{1:n}, y_{1:n})p(y_n|x_n)p(x_n|x_{n-1}),$$

and it follows that

$$p(x_{0:n}|y_{0:n}) = p(x_{0:n-1}|y_{0:n-1}) \frac{p(x_n|x_{n-1})p(y_n|x_n)}{p(y_n|y_{n-1})},$$
(4.5)

where $p(y_n|y_{n-1}) = \int p(x_{n-1}|y_{0:n-1})p(x_n|x_{n-1})p(y_n|x_n)dx_{n-1:n}$.

Most particle filtering methods are created by a numerical approximation to (4.5). A common and powerful algorithm is the SMC approximation. One can use a set of samples (particles) that are drawn from a posterior distribution to approximate the target posterior. More precisely, the posterior is the average calculated by

$$\hat{p}(x_{0:n}|y_{0:n}) = \frac{1}{N_p} \sum_{i=1}^{N_p} \delta_{x_{0:t}^i} \, \mathrm{d}x_{0:t}.$$

Here, $\{x_{0:t}^i\}_{i=1}^{N_p}$ are the particles and $\delta(d\cdot)$ is the standard delta function. As a result, when the

number of samples N_p is large enough, the average will approximate the true distribution. One of the advantages of the method is that one can prove the asymptotic convergence to the target distribution of interest. Besides, compared to some other approaches such as the extended Kalman filter and unscented Kalman filter, the SMC approach does not assume that the state models are Gaussian [9, 25]. One hence can apply the method in a broader area.

Unfortunately, it is not easy to draw samples from the posterior. An alternative way of drawing is to sample from a proposal distribution $q(x_{0:t}|y_{0:t})$ and to approximate the posterior using a weighted sum of particles. One usually calls this methodology the Bayesian important sampling.

Now, two questions remain unsolved. One is how to design a proposal distribution; another one is how to calculate the weight for each sample. How to select $q(x_{0:t}|y_{0:t})$ is an interesting research topic. One usually requires that the $q(x_{0:t}|y_{0:t})$ satisfies the following structure:

$$q(x_{0:t}|y_{0:t}) = q(x_{0:t-1}|y_{1:t-1})q(x_t|x_{0:t-1},y_{1:t}).$$

In this work, we are going to set $q(x_0|y_0) = p(x_0)$ and $q(x_t|x_{0:t-1}, y_{1:t}) = p(x_t|x_{t-1})$. According to [1, 12], if the latent variable dimension is not large and the observations are not too informative, setting the proposal to be equal to transition probability is good enough. To verify our method, we will conduct experiments with the transition probabilities $p(x_t|x_{t-1})$; the detailed design is shown in sections 4.4 and 4.5. The weights can then be calculated as follows:

$$w_t = w_{t-1} \frac{p(y_t|x_t)p(x_t|x_{t-1})}{q(x_t|x_{0:t-1},y_{1:t})},$$

and $w_1 = \frac{p(x_1)p(y_1|x_1)}{q(x_1|y_1)}$, where $p(y_t|x_t)$ is the likelihood. We omit the derivation, and one can refer to [1, 9, 25] for the details.

One issue of the algorithm is the degeneration of the weights; that is, the variance of the importance weights will become larger and larger with respect to time. Consequently, there are only a few samples that have a meaningful weight when *t* is large. One way to reduce the effect of degeneration is to use the resampling method. As a result, the algorithm is called sequential importance resampling (SIR). We provide a SIR algorithm in appendix A. There are various resampling methods; in this work, we apply systematic resampling as suggested in [9]; please check appendix A for the details.

4.2. Sources

In the next two subsections, we are going to demonstrate how we set up the testing problems. For equation (1.1), we set $\Omega = [0,1]^2$ and the terminal simulation time is T=0.1. Also $\kappa(x)$ is the given permeability which will be defined later in section 4.3, and the source $\sum_{k=1}^K p_k(x) \chi_{t \in [t_{k-1},t_k)}$ is partially known. More specifically, the time mesh grid $\{t_k\}_{k=0}^K$ is given, and the spatial components $\{p_k(x)\}_{k=1}^K$ are set to be characteristic functions. The kth source $p_k(x)$ is defined as:

$$p_k(x) = \begin{cases} p_k, & x \in A_k, \\ 0, & \text{otherwise,} \end{cases}$$
 (4.6)

Here p_k is a known constant; A_k is a square with a known size (is equal to 0.06×0.06 in all our experiments), but the location is not given. Our target work is to find one vertex coordinate of the A_k and k = 1, ..., K. One possible $p_k(x)$ is shown in figure 1 (left). In the following experiments, we will consider 2 sources. In both cases, K = 10 and $p_k = 1250$ for all k.

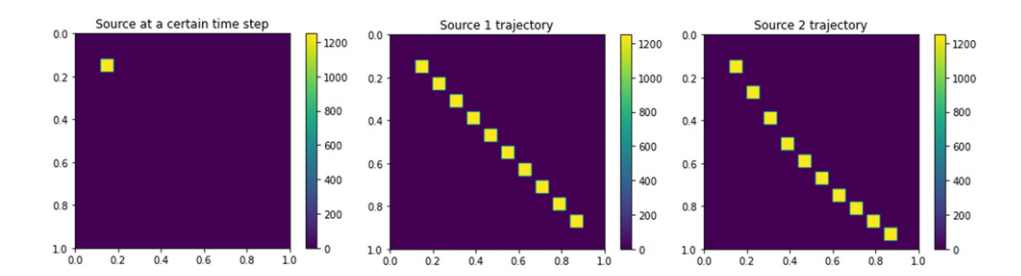


Figure 1. Demonstration of the source. Left: example of $p_k(x)$ which is the characteristic function defined in equation (4.6). The middle and right images show the trajectories of the source $\{p_k(x)\}_{k=1}^K$. Middle: source one, which is used in section 4.4. Right: source two, which is used in section 4.5.

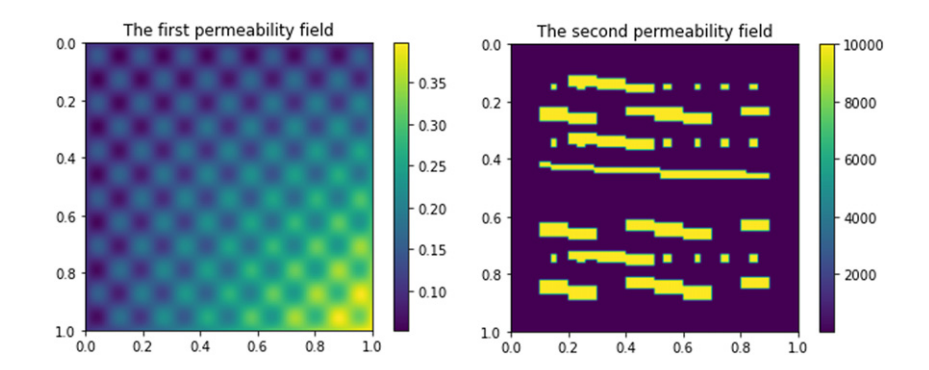


Figure 2. Left: the first permeability field 2D demonstration. $\max \kappa_1(x) = 0.3978$ and $\min \kappa_1(x) = 0.0521$. Right: the second permeability field 2D demonstration. The permeability in the yellow channels and dots equals 10^4 , while the permeability in the purple background is equal to 1.

We here list the vertices (left top) coordinates for both sources, and we will trace these two sequences of the coordinates later by our proposed method. The first list of vertices is: (0.12, 0.12), (0.20, 0.20), (0.28, 0.28), (0.36, 0.36), (0.44, 0.44), (0.52, 0.52), (0.60, 0.60), (0.68, 0.68), (0.76, 0.76), (0.84, 0.84); the second list of vertices is: (0.12, 0.12), (0.20, 0.24), (0.28, 0.36), (0.36, 0.48), (0.44, 0.56), (0.52, 0.64), (0.60, 0.72), (0.68, 0.78), (0.76, 0.84), (0.84, 0.90). For better illustration, we plot the trajectories of the two sources in figure 1, and we will discuss these two cases in sections 4.4 and 4.5 respectively.

4.3. Permeability fields

In equation (1.1), the operator \mathcal{A} includes the permeability field $\kappa(x)$. In order to better demonstrate the idea of the theorem and the algorithm, we will solve several multiscale problems. Two different permeability fields are used here. The first $\kappa_1(x)$ has multiple frequencies and is defined as follows:

Algorithm 1. Transition algorithm.

- 1 Input: current $x = (x_1, x_2)$
- 2 Initialize: set the size related parameters $r_1, r_2 > 0$ and speed related parameter s_0 , and draw a random number $s \sim \mathcal{U}(0, s_t)$. We then define $l_1 = s_0 + s + r_1$ and $l_2 = s_0 + s + r_2$
- 3 Create a rectangle: the top right vertex coordinate is $(x_1 + l_1\Delta x, x_2 + l_2\Delta x)$ and the size is equal to $(2r_1\Delta x, 2r_2\Delta x)$
- 4 Draw a point x' from the rectangle above uniformly; this point will be the next sample

```
\kappa_1(x, y) = 15 \sin(2\pi \cdot 0.01x) \cdot \sin(2\pi \cdot 0.05y) + 0.05 \sin(2\pi \cdot 6.5x) \cdot \sin(2\pi \cdot 6y) + 0.1
```

where $(x, y) \in \Omega := [0, 1]^2$ and it is demonstrated in figure 2 left.

The second permeability field $\kappa_2(x)$ (see figure 2 right for the illustration) has multiple high contrast channels and is widely used in the multiscale finite element method society [4, 6].

The multiple frequencies in $\kappa_1(x)$ and high contrast in $\kappa_2(x)$ bring difficulty in solving the corresponding equations numerically. We will use the standard finite element solver with spatial discretization $\Delta x = 10^{-2}$ in this work. For the temporal approximation, the backward Euler scheme is adopted, and the time discretization is $\Delta t = 10^{-3}$.

4.4. The first set of experiments

In this part, we present the first set of experiments whose source is defined in the middle image of figure 1. As we have discussed before, the proposal distribution q(x'|y',x) is the same with the transition probability p(x'|x) where x',y' denote the new sample and the observation of the next time step, respectively. We hence only need to specify p(x'|x), which is defined in algorithm 1.

Here we set $s_0 = 6$, $s_t = 5$ and $r_1 = r_2 = 4$. It should be noted that if one is given the exact current state $x = (x_1, x_2)$, the next exact state is $x' = (x_1 + 8\Delta x, x_2 + 8\Delta x)$ (please check the trajectory of the first source in section 4.2); however, the center (mean) of all proposed regions is deviated from the x'. This simulates the real-life scenario: one only knows the ship's route plan; however, the ship may depart from the original route, and one needs to find the real route, and positions when the ship leaks.

The observation is the flux of the boundary. For the multiple frequencies example, we measure the flux in the interval [0.45, 0.52] from each boundary; while for the high contrast permeability example, we only measure the flux in the interval [0.5, 0.55]. In both cases, the number of particles is 320. To evaluate our results, we calculate the mean of the samples at each time step k (this indicates the time step in the source) and compare it with the pre-set values. The demonstration and the relative error are shown in figure 3. We can see that the error decays in both examples. This is probably due to the error correction of the PF algorithm. The initial guess has a relatively large error, but the algorithm can correct the error by sampling from weighted samples whose weights are assigned by the algorithm. Starting from time step 6, the error is stabilized (figure 4).

4.5. The second set of experiments

In this set of experiments, we will use the second source, which is demonstrated as the right image in figure 1. We use the same transition algorithm in algorithm 1, but we use a different set of parameters, specifically, $s_0 = 4$, $s_t = 5$, $r_1 = 4$, $r_2 = 5$. Similar to the first source, all

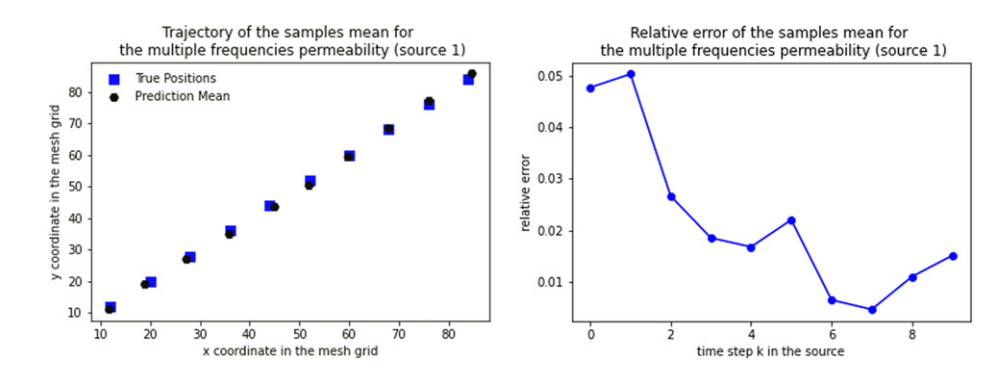


Figure 3. Samples mean and the relative error of the multiple frequencies' permeability with the first source. Left: samples mean and true source at each time step k. Right: relative error of the sample mean.

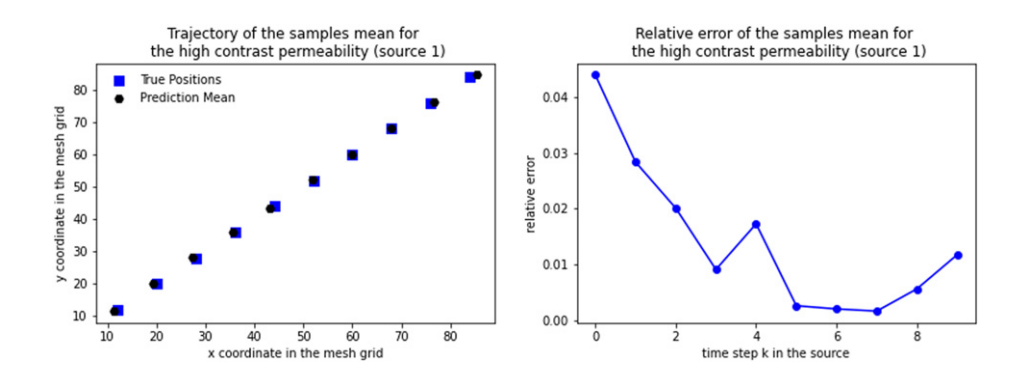


Figure 4. Samples mean and the relative error of the high contrast permeability with the first source. Left: samples mean and true source at each time step k. Right: relative error of the sample mean.

proposed regions' center (mean) deviates from x'. This is a real situation in which the ship's actual route is different from the original plan. The setting makes the predictions more challenging. For the flux measurement, we choose an interval [0.40, 0.60] from each boundary for the multiple frequencies permeability and [0.43, 0.58] from each boundary for the high contract permeability. The results are shown in figures 5 and 6, respectively. The error in figure 5 evolves similar as before. For figure 6, the error in the initial guess is already small enough, and hence it is fluctuating.

From the four examples presented above, we conclude that our algorithm is able to trace the exact source positions even if the proposal is far away from the exact route. The next challenge for us is to reduce the amount of observation data since by the theory, we can trace the source with flux on any open subset of the boundary. We will study this topic in the future.

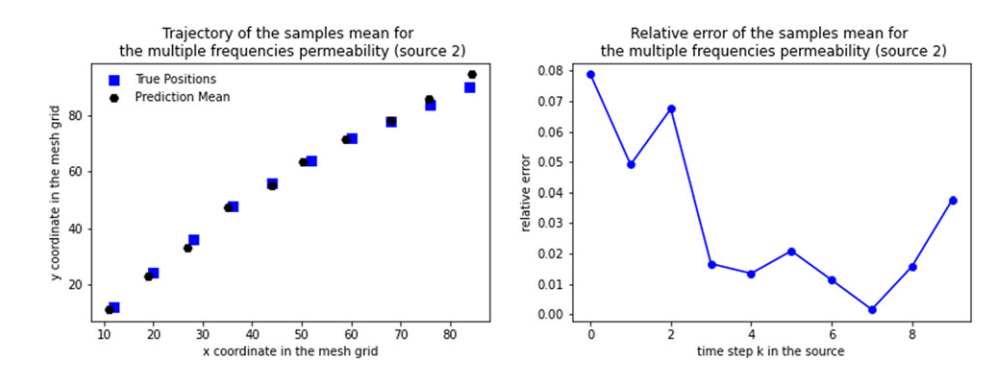


Figure 5. Samples mean and the relative error of the multiple frequencies' permeability with the second source. Left: samples mean and true source at each time step k. Right: relative error of the sample mean.

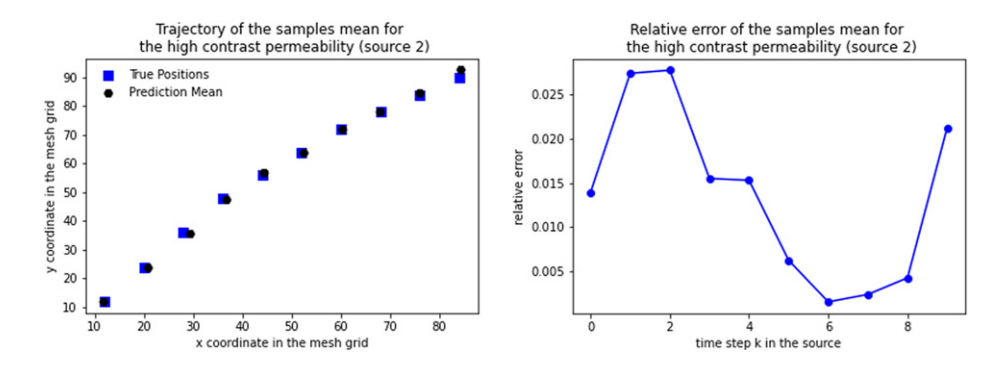


Figure 6. Samples mean and the relative error of the high contrast permeability with the second source. Left: samples mean and true source at each time step k. Right: relative error of the sample mean.

5. Concluding remarks and future works

This work considers the inverse source problem in the parabolic equation. The unknown source has a semi-discrete formulation, which can be used to approximate the general form F(x,t). We prove the uniqueness theorem—theorem 1, which says the data from any nonempty open subset of the boundary can support the uniqueness of the source. This conclusion is of significance in practical applications since it indicates that the source can be recovered from sparse boundary data and then save the cost. For the theoretical analysis, there is an interesting and meaningful work in the future: to determine the minimal observed area. Theorem 1 illustrates that the nonempty open subset of the boundary is sufficient to support the uniqueness. However, only from this theorem, we do not know whether we can minimize the observed area further. Finding the minimal observed area is one of our future works. Another exciting topic is to study a more general source format. For example, the source is not separable.

In the aspect of numerical reconstructions, since the model problem is a sequential prediction with a sequence of observations up to the time n, it is natural to formulate the problem as the Bayesian filtering problem. We apply one PF algorithm to solve the inverse problem with two multiscale permeabilities. Evaluating the likelihood function is the most time-consuming step, since it requires solving a forward problem with a fine resolution solver. We use the finite element solver in this work, however, the solver can be improved by the multiscale finite element solver or the deep learning solver. These solvers are more efficient meanwhile preserving accuracy, and we will study these topics in the future. We can also apply deep learning to train a solver. This is equivalent to solving the stochastic parametric PDE with the deep neural network. More precisely, we can train a mapping from the source to the flux on the boundary. One benefit of the method is that it will increase the computation efficiency in evaluating the likelihood function. Another benefit is that we can linearize the network; hence, more advanced PF algorithms can be used.

Furthermore, in this work, we only consider the case that the unknown $p_k(x)$ possesses the formulation (4.6) and the support A_k has a regular shape. The numerical reconstruction of the source with general formulation will be investigated in the future.

Acknowledgments

Guang Lin and Zecheng Zhang gratefully acknowledge the support of the National Science Foundation (DMS-1555072, DMS-1736364, DMS-2053746, and DMS-2134209), and Brookhaven National Laboratory Subcontract 382247, and US Department of Energy (DOE) Office of Science Advanced Scientific Computing Research program DE-SC0021142 and DE-SC0023161). Zhidong Zhang is supported by National Natural Science Foundation of China (Grant No. 12101627), and the Fundamental Research Funds for the Central Universities, Sun Yat-sen University (Grant No. 22qntd2901).

Data availability statement

The data that support the findings of this study are available upon reasonable request from the authors.

Appendix A. Particle filter algorithm

See algorithm 2.

Algorithm 2. Sequential importance resampling (SIR).

```
1 Initialize the number of time steps n and the number of particles N;
 2 Step 0: at t=0, draw the states x_0^i for i=1,...,N from the prior p(x_0);
 3 for t = 1, 2, ..., n do
        \mathbf{for}\ i=1,...,N\ \mathbf{do}
             Sample \hat{x}_t^i from the prior q(x_t|x_{0:t-1}^i,y_{1:t}) and extend the current trajectory by
 5
              adding the temporary proposed state \hat{x}^i_{0:t} = (x^i_{0:t-1}, \hat{x}^i_t);
             Calculate the importance weights recursively and normalize the resulting weights as
                                                  w_t^i = w_{t-1}^i \frac{p(y_t|\hat{x}_t^i)p(x_t^i|x_{t-1}^i)}{q(\hat{x}_t^i|x_{0:t-1}^i,y_{1:t})}.
        end
 7
        for i = 1, ..., N do
             Normalize the importance weights for the resampling purpose as
                                                           \tilde{w}_t^i = \frac{w_t^i}{\sum_{j=1}^N w_t^j}.
10
        Resampling: multiply samples \hat{x}^i_{0:t} with the normalized resampling weight \tilde{w}^i_t to obtain
11
          N random samples x_{0:t}^i which is roughly distributed following p(x_{0:t}^i|y_{1:t});
         Set w_t^i = \tilde{w}_t^i = \frac{1}{N} for all i = 1, ..., N;
12
        The algorithm will finally return a set of samples whose average is an approximation of
13
          the target distribution:
                                    p(x_{0:t}|y_{0:t}) \approx \hat{p}(x_{0:t}|y_{0:t}) = \frac{1}{N} \sum_{i=1}^{N} \delta_{(x_{0:t}^i)}(dx_{0:t}).
14 end
```

ORCID iDs

Guang Lin https://orcid.org/0000-0002-0976-1987 Zhidong Zhang https://orcid.org/0000-0003-0197-4889

References

- [1] Andrieu C, Doucet A and Holenstein H 2010 Particle Markov chain Monte Carlo methods J. R. Stat. Soc. B 72 269–342
- [2] Cannon J R 1968 Determination of an unknown heat source from overspecified boundary data source in the heat equation SIAM J. Numer. Anal. 5 275–86
- [3] Cheng J and Liu J 2020 An inverse source problem for parabolic equations with local measurements Appl. Math. Lett. 103 106213
- [4] Chetverushkin B, Chung E, Efendiev Y, Pun S-M and Zhang Z 2021 Computational multiscale methods for quasi-gas dynamic equations J. Comput. Phys. 440 110352
- [5] Chung E, Efendiev Y, Leung W T, Pun S-M and Zhang Z 2020 Multi-agent reinforcement learning accelerated MCMC on multiscale inversion problem (arXiv:2011.08954)
- [6] Chung E, Efendiev Y, Pun S-M and Zhang Z 2021 Computational multiscale methods for parabolic wave approximations in heterogeneous media (arXiv:2104.02283)

- [7] Douc R and Cappé O 2005 Comparison of resampling schemes for particle filtering ISPA 2005. Proc. 4th Int. Symp. Image and Signal Processing and Analysis, 2005 (Piscataway, NJ: IEEE) pp 64–9
- [8] Doucet A, Godsill S and Andrieu C 2000 On sequential Monte Carlo sampling methods for Bayesian filtering Stat. Comput. 10 197–208
- [9] Doucet A and Johansen A M 2011 A tutorial on particle filtering and smoothing: fifteen years later The Oxford Handbook of Nonlinear Filtering (Oxford: Oxford University Press) pp 656–704
- [10] Efendiev Y, Hou T and Luo W 2006 Preconditioning Markov chain Monte Carlo simulations using coarse-scale models SIAM J. Sci. Comput. 28 776–803
- [11] Folland G B 1992 Fourier Analysis and Its Applications (The Wadsworth & Brooks/Cole Mathematics Series) (Pacific Grove, CA: Wadsworth & Brooks/Cole Advanced Books & Software)
- [12] Gordon N, Salmond D J and Smith A F M 1993 Novel approach to nonlinear/non-Gaussian Bayesian state estimation *IEE Proc. F (Radar and Signal Processing)* vol 140 (IET) pp 107–13
- [13] Hettlich F and Rundell W 2001 Identification of a discontinuous source in the heat equation *Inverse Problems* 17 1465–82
- [14] Huang X, Imanuvilov O Y and Yamamoto M 2020 Stability for inverse source problems by Carleman estimates *Inverse Problems* 36 125006
- [15] Ikehata M 2007 An inverse source problem for the heat equation and the enclosure method *Inverse Problems* 23 183–202
- [16] Isakov V 1990 Inverse Source Problems Mathematical Surveys and Monographs vol 34 (Providence, RI: American Mathematical Society)
- [17] Jin B, Kian Y and Zhou Z 2021 Reconstruction of a space-time-dependent source in subdiffusion models via a perturbation approach SIAM J. Math. Anal. 53 4445–73
- [18] Jouin M, Gouriveau R, Hissel D, Péra M-C and Zerhouni N 2016 Particle filter-based prognostics: review, discussion and perspectives *Mech. Syst. Signal Process.* **72–73** 2–31
- [19] Li Z and Zhang Z 2020 Unique determination of fractional order and source term in a fractional diffusion equation from sparse boundary data *Inverse Problems* 36 115013
- [20] Lin G, Wang Y and Zhang Z 2021 Multi-variance replica exchange stochastic gradient MCMC for inverse and forward Bayesian physics-informed neural network (arXiv:2107.06330)
- [21] Walter R 1976 Principles of mathematical analysis International Series in Pure and Applied Mathematics 3rd edn (New York: McGraw-Hill)
- [22] Rundell W and Zhang Z 2018 Recovering an unknown source in a fractional diffusion problem J. Comput. Phys. 368 299–314
- [23] Rundell W and Zhang Z 2020 On the identification of source term in the heat equation from sparse data *SIAM J. Math. Anal.* **52** 1526–48
- [24] Stuart A M 2010 Inverse problems: a Bayesian perspective Acta Numer. 19 451–559
- [25] Van Der Merwe R, Doucet A, De Freitas N and Wan E 2000 The unscented particle filter Adv. Neural Inf. Process. Syst. 13
- [26] Yamamoto M 2009 Carleman estimates for parabolic equations and applications *Inverse Problems* **25** 123013